NAVAL POSTGRADUATE SCHOOL
Monterey, California

THESIS

EXPERIMENTAL AND NUMERICAL INVESTIGATION OF SECOND-GENERATION, CONTROLLED-DIFFUSION, COMPRESSOR BLADES IN CASCADE

by

Darren V. Grove

June, 1997

Thesis Advisor: Garth V. Hobson

Approved for public release; distribution is unlimited.

REPORT DOCUMENTATION PAGE

Form Approved OMB No. 0704-0188

1. AGENCY USE ONLY *(Leave blank)*	2. REPORT DATE June 1997	3. REPORT TYPE AND DATES COVERED Master's Thesis

4. TITLE AND SUBTITLE
Experimental and Numerical Investigation of Second-Generation, Controlled-Diffusion, Compressor Blades in Cascade

5. FUNDING NUMBERS

6. AUTHOR(S) Darren V. Grove

7. PERFORMING ORGANIZATION NAME(S) AND ADDRESS(ES)
Naval Postgraduate School
Monterey, CA 93943-5000

8. PERFORMING ORGANIZATION REPORT NUMBER

9. SPONSORING / MONITORING AGENCY NAME(S) AND ADDRESS(ES)

10. SPONSORING / MONITORING AGENCY REPORT NUMBER

11. SUPPLEMENTARY NOTES
The views expressed in this thesis are those of the author and do not reflect the official policy or position of the Department of Defense or the U.S. Government.

12a. DISTRIBUTION / AVAILABILITY STATEMENT
Approved for public release; distribution unlimited.

12b. DISTRIBUTION CODE

13. ABSTRACT *(maximum 200 words)*

This thesis contains a detailed experimental and numerical investigation of second-generation, controlled-diffusion, compressor-stator blades at an off-design inlet-flow angle of 39.5°. Investigation of the blades took place in a low-speed cascade wind tunnel using various experimental procedures. The objective of the wind tunnel study was to characterize the flow field in and around the blades at the off-design angle, and to investigate flow separation near the mid-chord for a high Reynolds number of 640,000. Rake probe survey's were performed upstream and downstream of the blades in order to obtain spanwise total pressure profiles. Surface flow visualization was performed on the blades using a titanium dioxide and kerosene mixture. Blade surface pressure measurements were obtained using a 40-hole instrumented blade from which coefficients of pressure were calculated. A standard optics, two-component, laser-Doppler velocimeter was used to characterize the flow field upstream, in the boundary layer on the suction side of the blades, and in the wake region. A numerical investigation was conducted using the rotor viscous code 3-D developed by Dr. Roderick Chima of NASA Lewis Research Center. Overall, good agreement between flow visualization, blade pressure measurements, laser measurements, and numerical modeling was obtained.

14. SUBJECT TERMS

15. NUMBER OF PAGES

16. PRICE CODE

17. SECURITY CLASSIFICATION OF REPORT	18. SECURITY CLASSIFICATION OF THIS PAGE	19. SECURITY CLASSIFICATION OF ABSTRACT	20. LIMITATION OF ABSTRACT
Unclassified	Unclassified	Unclassified	UL

NSN 7540-01-280-5500

Standard Form 298 (Rev 2-89)
Prescribed by ANSI Std. 239-18

Approved for public release; distribution is unlimited.

EXPERIMENTAL AND NUMERICAL INVESTIGATION OF SECOND-GENERATION, CONTROLLED-DIFFUSION, COMPRESSOR BLADES IN CASCADE

Darren V. Grove
Aeronautical Performance Engineer, Naval Air Systems Team
B.S.A.E., University of Maryland, 1993

Submitted in partial fulfillment of the
requirements for the degree of

MASTER OF SCIENCE IN AERONAUTICAL ENGINEERING

from the

NAVAL POSTGRADUATE SCHOOL
June 1997

Author: Darren Grove
Darren V. Grove

Approved by: Garth V. Hobson
Garth V. Hobson, Thesis Advisor

Raymond P Shreeve
Raymond P. Shreeve, Second Reader

Daniel J. Collins
Daniel J. Collins, Chairman
Department of Aeronautics and Astronautics

ABSTRACT

This thesis contains a detailed experimental and numerical investigation of second-generation, controlled-diffusion compressor-stator blades at an off-design inlet-flow angle of 39.5°. Investigation of the blades took place in a low-speed cascade wind tunnel using various experimental procedures. The objective of the wind tunnel study was to characterize the flow field in and around the blades at the off-design angle, and to investigate flow separation near the mid-chord for a high Reynolds number of 640,000. It was known from previous studies that boundary layer thickness on the end walls were of different thicknesses. Thus, prior to taking data, an adjustment to the end wall boundary layer thickness was attempted by insertion of an aluminum trip strip far upstream of the blades. Rake probe survey's were performed upstream and downstream of the blades in order to obtain spanwise upstream and downstream total pressure profiles. Surface flow visualization was performed on the blades using a titanium dioxide and kerosene mixture. Blade surface pressure measurements were obtained using a 40-hole instrumented blade from which coefficients of pressure were calculated. A standard optics, two-component laser-Doppler velocimeter was used to characterize the flow field upstream, in the boundary layer on the suction side of the blades, and in the wake region. A numerical investigation was conducted using the rotor viscous code 3-D developed by Dr. Roderick Chima of NASA Lewis Research Center.

Overall, good agreement between flow visualization, blade pressure measurements, laser measurements, and numerical modeling was obtained.

TABLE OF CONTENTS

LIST OF FIGURES

LIST OF SYMBOLS

c	blade chord
$c_{uv} = \dfrac{\overline{u'v'}}{\sqrt{\overline{u'}^2}\sqrt{\overline{v'}^2}}$	Reynolds stress correlation coefficient
c_{ac}	% blade axial chord
C_N	coefficient of blade force normal to the chord
$C_p = (P_l - P_\infty)/(p_{t\infty} - P_\infty)$	coefficient of pressure
d	distance normal to the blade surface
$P_{hub\ exit} / P_o$	hub exit pressure to inlet reference pressure
P_l	local static pressure
P_s	Prandtl static pressure
P_t	Prandtl total pressure
Re	Reynolds number
S	blade pitch/spacing
$T_u = \dfrac{\sqrt{\overline{u'}^2}}{V_{ref}}$	axial turbulence intensity
$T_v = \dfrac{\sqrt{\overline{v'}^2}}{V_{ref}}$	tangential turbulence intensity
U	axial velocity component
u'	axial fluctuating velocity
$\overline{u'v'}$	Reynolds stress
V	tangential velocity component
V_{ref}	inlet reference velocity
v'	tangential fluctuating velocity
$W = (U^2 + V^2)^{1/2}$	total velocity
x	axial direction
y	tangential direction
β_1	tunnel inlet flow angle
β_{1w}	tunnel sidewall setting angle
β_2	tunnel outlet angle
β_{2w}	tunnel tailboard setting angle
$\delta = \dfrac{c}{S}$	blade solidity
η	axis normal to blade chord
ξ	axis tangent to blade chord

ACKNOWLEDGEMENTS

I would like to extend my sincere appreciation to Associate Professor Garth Hobson and Professor Raymond Shreeve for their enthusiasm and technical guidance in helping make one of my dreams an achievement. Their in-depth knowledge about the subject of turbomachinery is proof of their dedication towards teaching others. I am glad to have had the opportunity to work with both of them.

I would like to acknowledge and give thanks to Janet Sabo, of the Naval Aviation Executive Institute, and to the propulsion and power team at Naval Air Systems Command for giving me the financial support to obtain my degree. Also, I would like to thank my immediate supervisor, Mel Luter, for his support, and allowing me time off from my normal duties to finish my degree at the Naval Postgraduate School.

Lastly, I would like to thank my family for believing in me. You have made some rough times smooth and helped me to believe in myself. And to my belated Father, who has taught me to work hard and take pride in what I do, to you I owe my gratitude for giving me a great life.

I. INTRODUCTION

A. BACKGROUND

For many years, jet engines have been limited by compressor stall and off-design performance behavior. Compressor stall can lead to degradation of engine performance and possibly the loss of the engine. Research and development over the past few decades has worked towards increasing engine blade performance. With new advances in compressor blade design technology, such as computational fluid dynamics (CFD) analysis, the goal is to improve engine performance by allowing higher blade loading while still maintaining stall margin and efficiency. For these reasons, a new generation of controlled-diffusion (CD) blading was developed.

Controlled-diffusion (CD) blading is shaped such that higher angles of incidence may be achieved before boundary layer separation occurs, thus increasing the blade loading. This is done by designing the blade to control the diffusion on the suction side so as to avoid boundary layer separation. Higher blade loading will allow more turning of the air flow for a given number of blades (or solidity), or the same turning with fewer blades (lower solidity). Therefore, fewer blades will be required to produce the same compression ratio which will result in a lower engine weight and better performance.

The present study conducted at the Naval Postgraduate School (NPS) low-speed cascade wind tunnel (LSCWT) involved the CD compressor stator blades 67B, designed by Thomas F. Gelder of NASA Lewis Research Center [Ref. 1]. stator 67B, together with rotor 67, comprise compressor stage 67B. The 67B stator blades were second-generation CD blades designed as an improvement over the former 67A first-generation blades, designed by Nelson Sanger [Ref. 2]. Prior to the study, ten midspan stator 67B compressor blades were machined from aluminum and installed in the LSCWT.

Previous studies were done on the blades at a design inlet flow angle of 36.3° by Hansen [Ref. 3], and at an off-design inlet flow angle of 38.0° by Schnorenberg [Ref. 4].

B. PURPOSE

The objective of the present study was to characterize the flow pattern upstream, in the passages between the blades, in the boundary layer of the blades, and in the wake region at an inlet flow angle of 39.5° at a Reynolds number of 640,000. Also, a detailed investigation was to be performed on the separation region which occurred near mid-chord. Various methods were to be used, including flow visualization, rake probe surveys, blade surface pressure measurements, and laser-Doppler velocimetry (LDV) measurements. A adjustment was made to the wind tunnel wall boundary layer prior to taking data to obtain improved spanwise symmetry over the blade. A numerical investigation using 3-D CFD was also conducted and the predictions were compared with the experimental results.

II. TEST FACILITY AND SETUP

A. LOW-SPEED CASCADE WIND TUNNEL

The low-speed cascade wind tunnel is located at the NPS Turbopropulsion Laboratory facilities. The wind tunnel is powered by a 750 hp electric motor driving a turbo-vane blower, and is capable of producing a sustained maximum free-stream Mach number of .4 in the test section. Figure 1 shows a schematic of the LSCWT in the Low Speed Turbomachinery Building (Bldg. 213) with the associated plenum chamber, drive system, and inlet and exhaust ducting. Hansen [Ref. 3] gave a detailed description of the test facility and test section. Tunnel flow conditions were documented for uniformity and periodicity in the cascade test section using 20 Stator 67A blades at approximately 40.0° (design), 43.0° and 46.0° inlet flow angle by Elazar [Ref. 5].

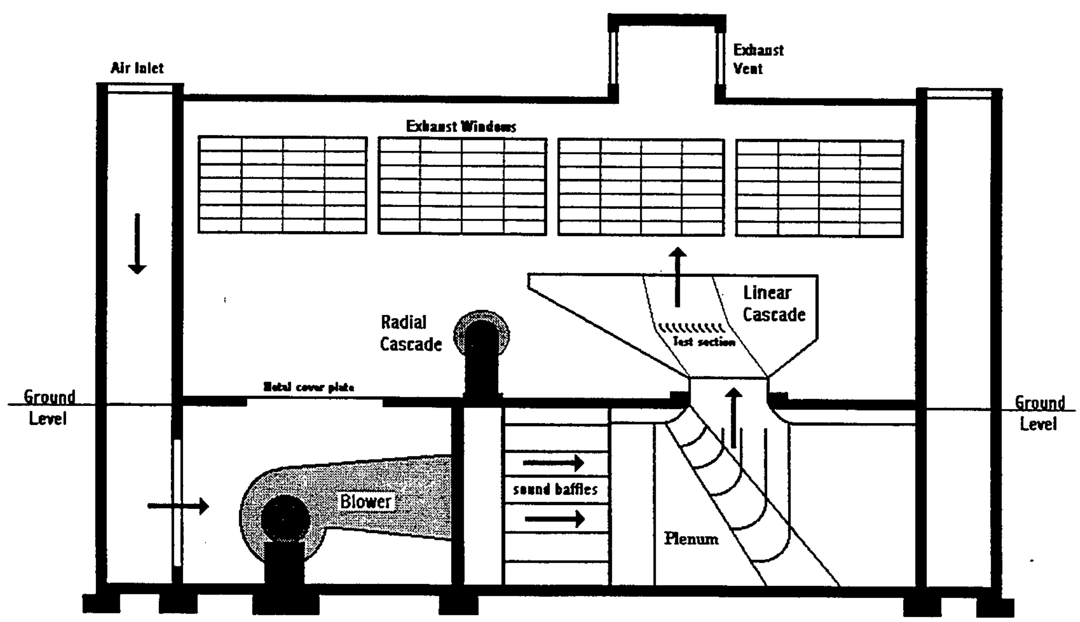

Figure 1. NPS Cascade Wind Tunnel Facility.

B. TEST SECTION

Figure 2 shows the layout of the LSCWT and test section with dimensions. Prior to the present study, 10 stator 67B CD blades were installed in the test section and tested at the design inlet flow angle of 36.3° by Hansen [Ref. 3], and at 38° by Schnorenberg [Ref. 4]. Reference 4 contains a description of the procedure to adjust the inlet flow angle. As can be seen in Figure 2, air was forced up through the 60 inlet guide vanes were it was turned towards the test section. The flow then entered the test section and was once again turned vertically, and finally exited to ambient pressure.

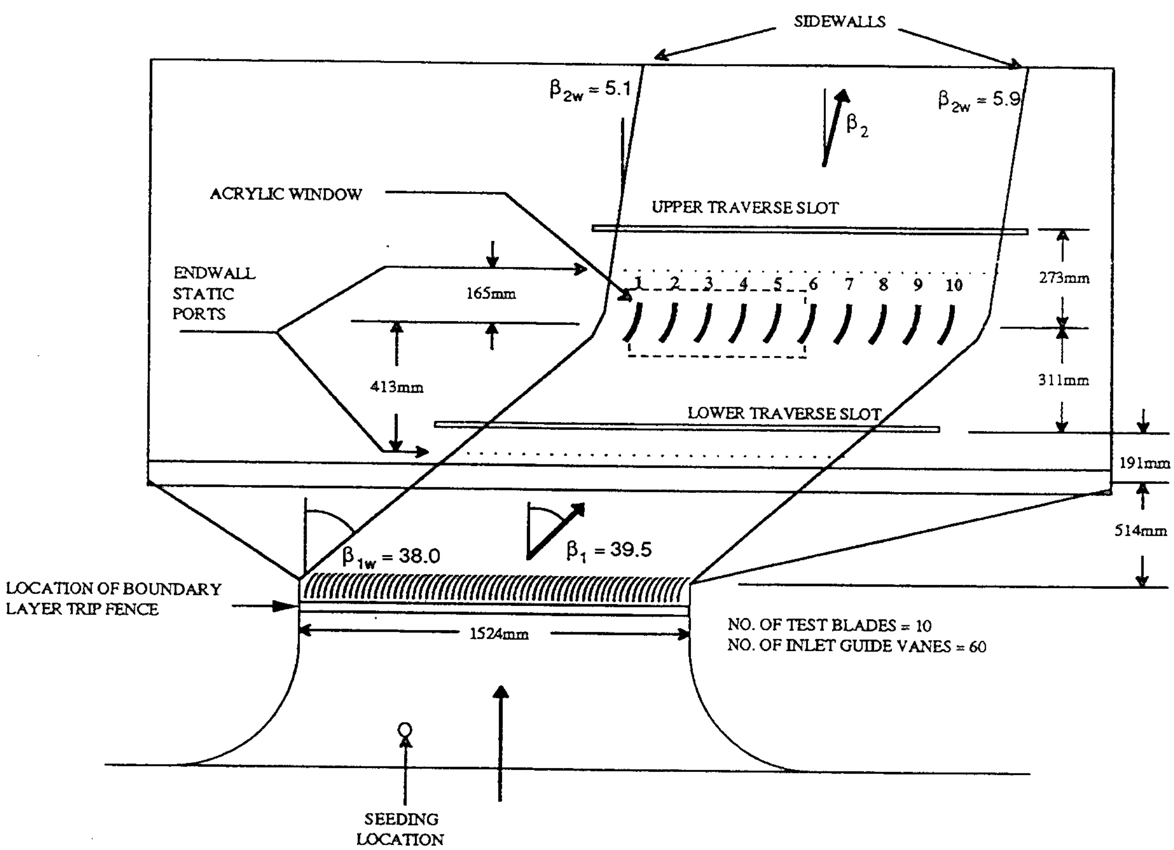

Figure 2. Detailed Schematic of Test Section.

Each blade had a chord length of 127.25 mm (5.01 in), and a span of 254 mm (10.0 in). The blades were separated in the pitch-wise direction by 152.4 mm (6.0 in). Figure 3 below shows a detailed profile of the 67B stator blade. Test section data are summarized in Table 1.

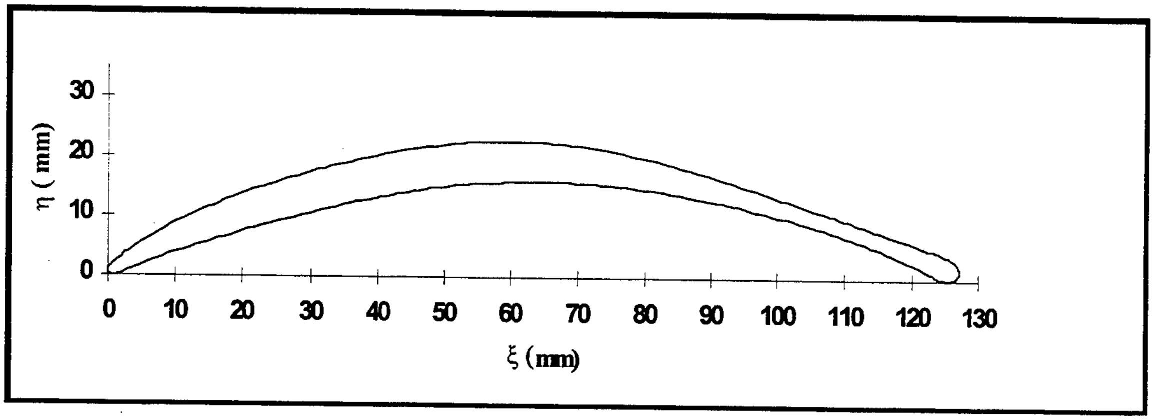

Figure 3. Stator 67B Blade Profile.

Tunnel Span	**254 mm (10 in.)**
Blade Type	**Stator 67B Controlled-Diffusion**
Blade material	**Aluminum**
Number of Blades	**10**
Blade spacing	**152.4 mm (6 in.)**
Chord	**127.14 mm (5.01 in.)**
Solidity	**0.834**
Thickness/Chord	**0.05**
Setting Angles	**16.3° ± 0.1°**

Table 1. Test Section Data.

Two partially instrumental blades containing 8 pressure taps each, were installed at locations 2 and 8 (Fig. 2), while a third fully-instrumented blade containing 42 pressure taps was installed at location 6. Blades 3 and 4 were treated with a black anodized coating to minimize laser light scatter for LDV measurements and were also used for flow visualization.

Eight survey stations based on axial chord length that were used for the study. Figure 4 shows the distances from the leading edge as a fraction of the blade axial chord. The station numbering system was consistent with earlier studies.

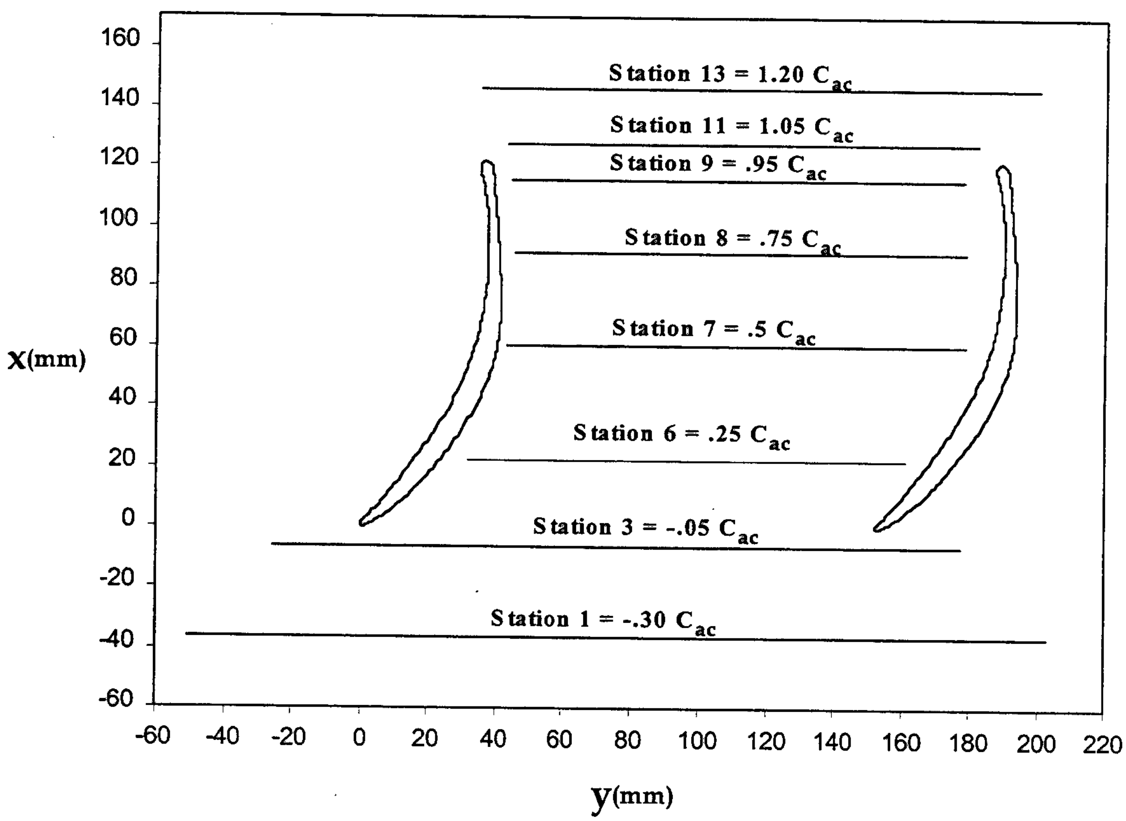

Figure 4. Survey Stations and Numbering in Terms of Axial Chord.

1. Wall Boundary Layer Adjustment

It was shown by Webber [Ref. 6] using upstream rake probe surveys that the boundary layer thickness on the north wall of the wind tunnel was thicker than on the south wall. At high Reynolds number, Schnorenberg [Ref. 4] recorded flow separation with 3-D vortices that were not symmetrical with respect to blade chord length. Furthermore, the core flow was displaced towards the south wall by the north wall boundary layer, making the flow non-symmetrical about the midspan of the blade.

The objective of the wall boundary layer adjustment was to improve the flow symmetry about the midspan of the blade. A 1.5875 millimeter (1/16in.) thick, by 15.875 millimeter (5/8in.) wide, by 1524 millimeter (60in.) aluminum trip strip was inserted into the flow on the south wall just upstream of the 60 inlet guide vanes. Figure 5 shows the schematic of the aluminum trip strip inserted into a holding frame. The strip caused a thicker boundary layer to form on the south wall, thus displacing the flow back to be more symmetrical about the midspan. By doing so, the endwall corner vorticies were also found to be of the same size, and at the same distance from the leading edge.

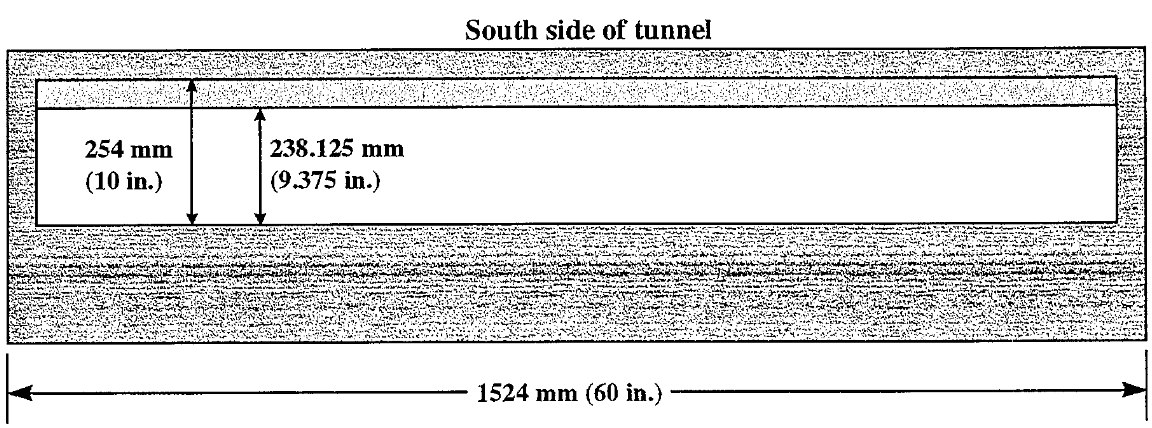

Figure 5. Aluminum Boundary Layer Trip Strip in Wooden Frame.

C. INSTRUMENTATION SETUP

1. Flow Visualization

Blade surface flow visualization was performed using a titanium dioxide (TiO_2) and kerosene mixture. The flow patterns on the surface of the blades were recorded using an 8mm video camera. Black and white photographs were taken after the solution dried on the blades to show the final results. The steps for mixing the solution are in given Appendix A.

2. Blade Surface Pressure Measurements

Surface pressure measurements were recorded using a 48 channel pneumatic Scanivalve rotary system controlled by a HP-9000 computer. The software to control the system was fully documented by Classick [Ref.7], and later modified by Armstrong [Ref.8]. Scanivalve ports and channel assignments are shown in Table C1 in Appendix B.

3. Rake Probe Measurements

A 20-hole rake probe was used to acquire pitch-wise surveys of the spanwise distribution of coefficient of pressure C_p upstream and downstream of the blades. The rake probe consisted of 17 total pressure ports, 1 static pressure port, and 2 yaw ports. Figure 6 shows a schematic of the probe along with an upstream survey diagram showing position and traverse direction. Here again, data were recorded using a 48 channel pneumatic Scanivalve rotary system controlled by a HP-9000 computer. Scanivalve ports and channel assignments are shown in Table C2 in Appendix B.

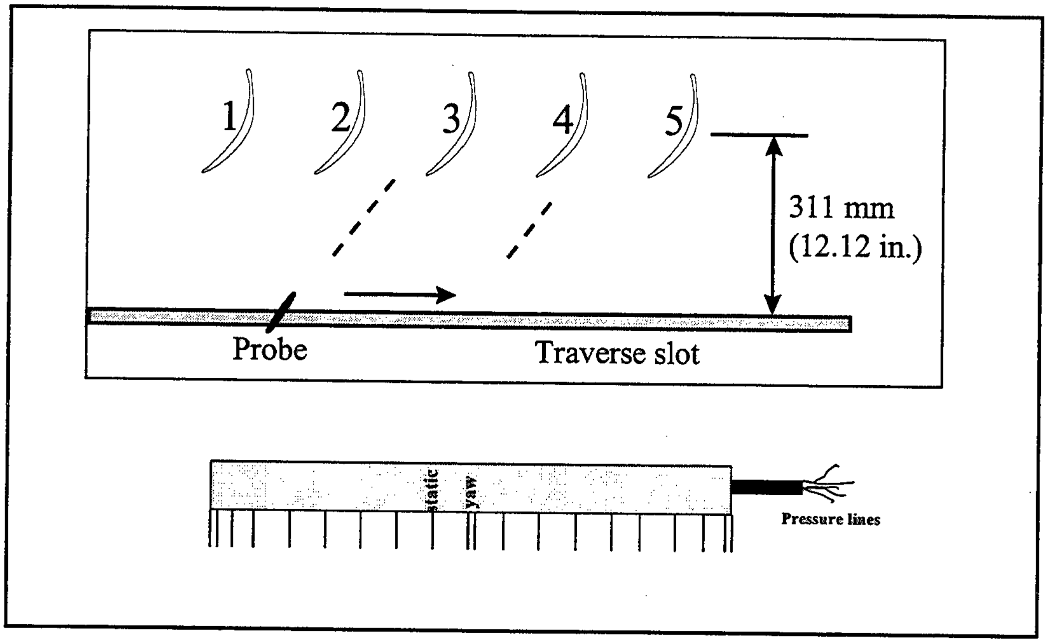

Figure 6. Upstream Survey Schematic and Rake Probe.

4. LDV Measurements

LDV measurements were obtained using a four-beam, two-color TSI Model 9100-7 system. A description of the setup, including optics, atomizer seeding, and laser type are thoroughly described by Elazar [Ref. 5]. Data acquisition and the traverse mechanism were controlled by a personal computer (PC) using TSI Flow Information Display (FIND) Software (version 4.0). Software inputs used for the present study are given in Appendix C. The data acquisition and traverse mechanism are described in detail by Murray [Ref. 9]. The LDV laser and traverse table are shown in Figure 7.

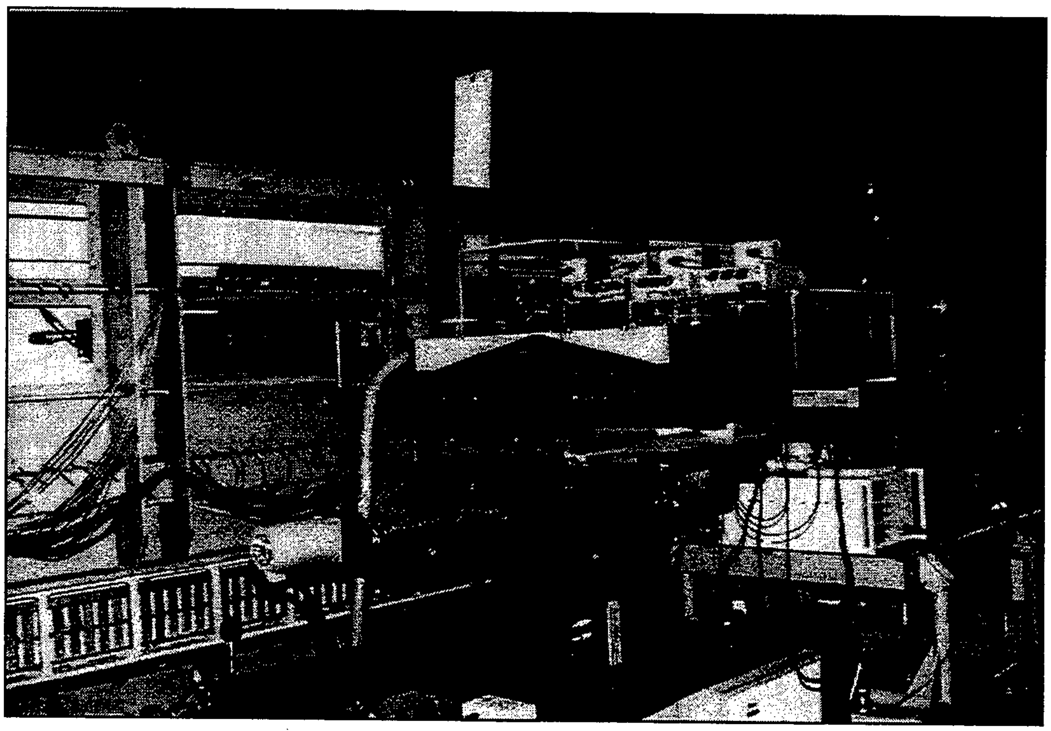

Figure 7. LDV, Traverse Table, and Cascade Test Section.

III. EXPERIMENTAL PROCEDURE

A. WALL BOUNDARY LAYER ADJUSTMENT

Various methods such as meshed screens (with different types of fineness), honeycomb screens, and flow straighteners have been used to adjust inlet flows and to make them more uniform. The procedure tried here was to insert various widths of aluminum strips into the flow field on the south side of the wind tunnel wall, just upstream of the 60 inlet guide vanes so as to make the flow on the blade surface more symmetrical in the spanwise direction. After installation of the aluminum boundary layer trip strip, a titanium dioxide and kerosene solution was brushed onto blades 3, 4, and 5. The wind tunnel was started and allowed to stabilize at a test section speed of Mach .22 ($\cong$ 70.0 m/s). Surface flow visualization was used to record the flow transient and steady-state flow patterns on the blades. This procedure was done repeatedly for various widths of aluminum strips. It was found that a 15.875 mm protrusion of an aluminum strip into the airflow gave symmetrical flow about the blades, which appeared to be symmetrical in the spanwise direction.

B. WIND TUNNEL CALIBRATION

During the calibration runs, the wind tunnel was allowed to reach a plenum temperature equilibrium for each speed. The tunnel was run at 7 different speed settings (plenum pressure), 78.74 mm (3.1 in.), 114.3 mm (4.5 in.), 147.32 mm (5.8 in.), 203.2 mm (8.0 in.), 254 mm (10.0 in.), 304 mm (12.0 in.), and 355.6 mm (14.0 in.) of H_20. Plenum pressure, plenum temperature, and ambient pressure were recorded. Using the LDV, horizontal (U) and vertical (V) velocities components were recorded for each speed. The data were used in a FORTRAN program , CALIB1.FOR, which fit the tunnel characteristics using a least-squares method to determine the pressure ratio as a function of Mach number [Ref. 3].

C. FLOW VISUALIZATION

Surface flow visualization was performed using a titanium dioxide (TiO_2) and kerosene mixture. Mixing procedures are given in Appendix A. With the acrylic window removed, the mixture was applied evenly on blades 3, 4, and 5 with a fine-hair paint brush. The acrylic window was immediately reinstalled and the wind tunnel was started. The tunnel was bought up to a speed of Mach .22 in the test section. An 8mm VHS video camera mounted on a tripod was used to record the transient and final flow field patterns on the blades. All test section flow conditions corresponded to a Reynolds number of 640,000.

D. LDV MEASUREMENTS

1. Probe Volume Alignment

Prior to each survey, the probe volume formed by the intersecting laser beams was aligned with an aluminum alignment tool. Details on alignment procedures are described in reference 4. All surveys were done at midspan of the blades.

2. LDV Surveys

The LDV was aligned and leveled such that the X, Y, Z, traverse motions would move the measurement volume horizontal (blade-to-blade), vertical (normal to the leading edge locus), and parallel (spanwise to the blade), for surveys taken at stations 1 through 13. For station 3, the laser was pitched up 5°, while at station 11, the laser was pitched down 5°, in order to avoid interference of the blue beam with the leading and trailing edge respectively. For all boundary layer surveys, the laser was yawed 4° to the left in order to avoid interference of the green beam with the end tip of the blade. A total of 12 LDV survey's were done at an off-design inlet flow angle of 39.5° for a Reynolds number of 640,000. Boundary layer surveys were completed on blade #3 with station 8 repeatability measurements on blade #4. Inlet flow surveys were done at stations 1 and 3, while wake survey's were done at stations 11 and 13. With the measurements taken in coincidence mode, a total of 1000 data points were collected for each sample point. Axial (vertical) velocities U, were recorded using the 514.5 nm green beams, while tangential (horizontal) velocities V, were recorded using the 488 nm blue beams. Fringe spacing based on half-angle calculations gave 4.7569 microns for the green beam , and 4.5119 microns for the blue beam. A 5 Mhz frequency shift was used to detect flow reversal.

For each survey, plenum total pressure (P_{to}) , plenum total temperature (T_{to}), and ambient pressure (P_{amb}) were recorded. Program CALIB1.FOR [Hansen, Ref. 3], used P_{to}, T_{to}, and P_{amb} to calculate the tunnel inlet reference velocity (V_{ref}) for each survey. V_{ref} is then used to non-dimensionalize the total velocity (W), axial velocity (U), tangential velocity (V), and, U and V turbulence intensities, so that individual surveys could be compared. Appendix D lists the non-dimensionalized data for each survey.

IV. RESULTS AND DISCUSSION

A. FLOW VISUALIZATION

Results show that after the boundary layer trip strip was inserted into the upstream flow field on the south wall of the tunnel, the inlet flow was more symmetrical about the midspan of the blades. Figures 8 and 9 show, for comparison, Schnorenberg's [Ref. 4] results and the present results, respectively. For the present study, two counter-rotating vortices appeared at approximately .78 $C_{ac.}$. These vortices were the result of corner vortices which formed due to the interaction of the endwall boundary layer with the blade leading edge. Both vortices were symmetric about the spanwise direction, and located at the same chordwise position.

Measurements taken from the photographs showed that separation of the flow occurred at .5 C_{ac} at the midspan of the blades. The separation line was not straight along the span of the blade because of the three-dimensional endwall effects. Actual separation of the boundary layer was most probably farther downstream because of the gravitational effects of the titanium dioxide and kerosene mixture.

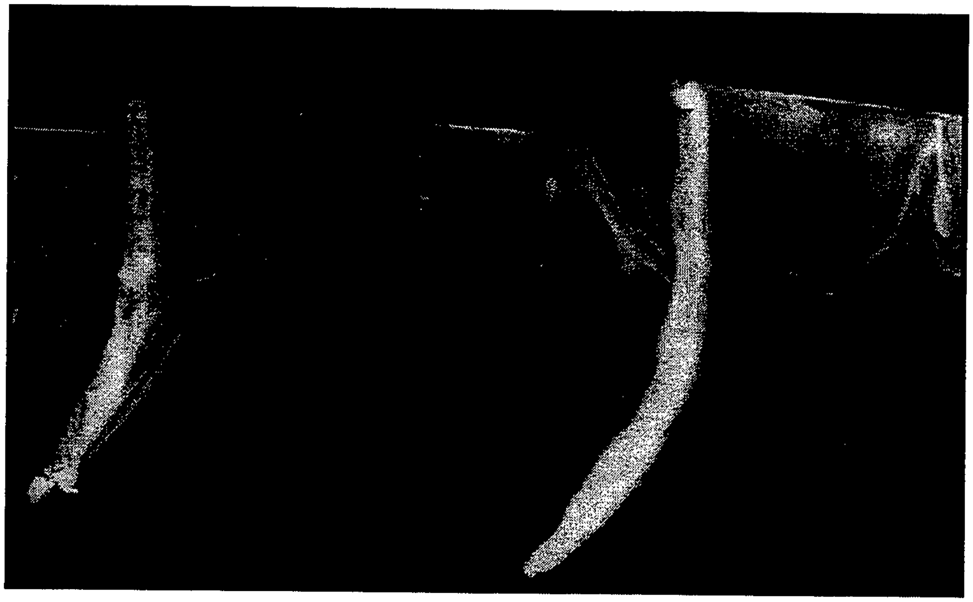

Figure 8. Previous Result without Boundary Layer Trip Strip.

Figure 9. Result with Boundary Layer Trip Strip.

Flow visualization also showed excellent periodicity between blades 3, 4, and 5. Figure 10 is a photograph taken of blades 3 and 4 to show how periodic the flow was from blade to blade. An averaged 5% difference was measured between the locations of the vortices and separation points between blades 3, 4, and 5.

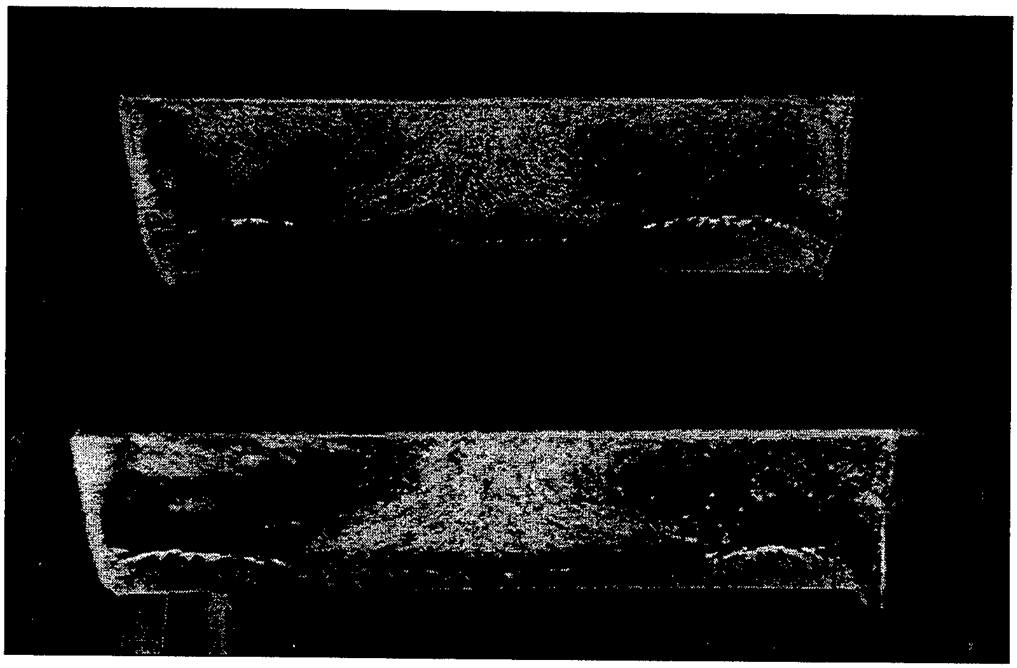

Figure 10. Flow Visualization Periodicity study.

B. BLADE SURFACE PRESSURE MEASUREMENTS

Blade surface pressure measurements were taken on blade 6 at the high Reynolds number. Figure 11 below shows the results of the pressure distribution in terms of the coefficient of pressure, C_p, vs fraction of blade chord (ξ/c).

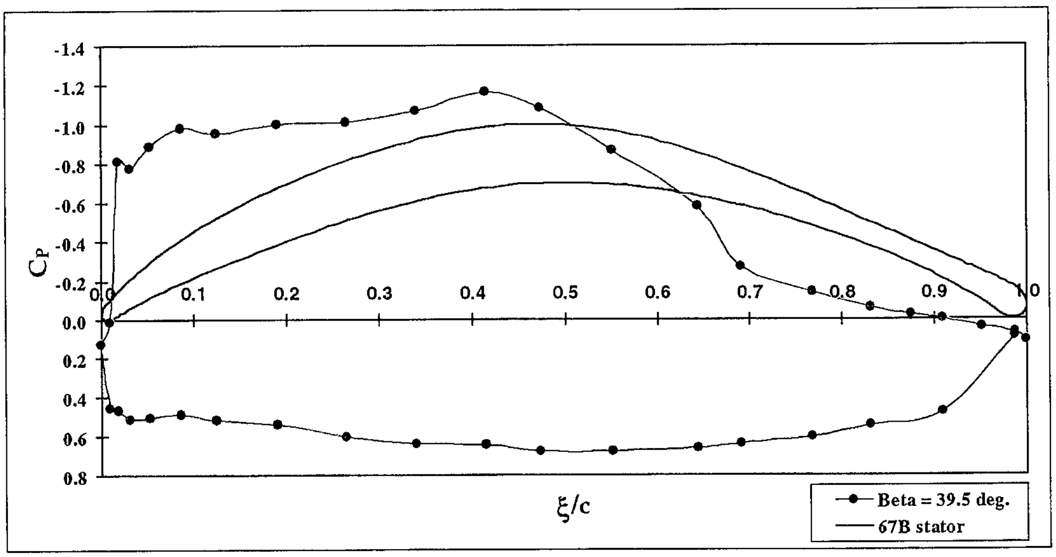

Figure 11. C_p vs ξ/c for Beta = 39.5°.

For the suction side of the blade, C_p is shown to decrease to -0.8 almost immediately about the leading edge. The diffusion between suction point 2 and 3 may be an indication of a leading edge separation bubble. Re-acceleration of the flow continues to 0.4 ξ/c where a minimum C_p of -1.17 was reached. This point corresponded to a maximum Mach number of .345. From 0.4 ξ/c the C_p distribution gradually increased linearly to 0.64 ξ/c which showed no sign of flow separation. However, between 0.64 and 0.69 ξ/c a severe adverse pressure gradient existed causing turbulent flow separation on the blade. The C_p distribution over most of the pressure surface was constant, except at the trailing edge. The jump in C_p was caused by a reverse flow aft of the blunt trailing edge of the blade.

A comparison was made of the on-design and two off-design angles of incidence. On-design blade pressure measurements were obtained by Hansen [Ref. 3] at 36.3°, while Schnorenberg [Ref. 4] performed measurements at 38.0° inlet flow angle. Figure 12 shows the comparison of the results. Overall, they compared well. The current study, at 39.5°, showed that for the region between 0.0 and 0.4 ξ/c , a higher blade loading occurred with a possible separation bubble at the leading edge. After 0.4 ξ/c a slightly higher diffusion rate was seen with strong diffusion between 0.64 ξ/c and 0.69 ξ/c. No significant differences were noted for the pressure side of the blade.

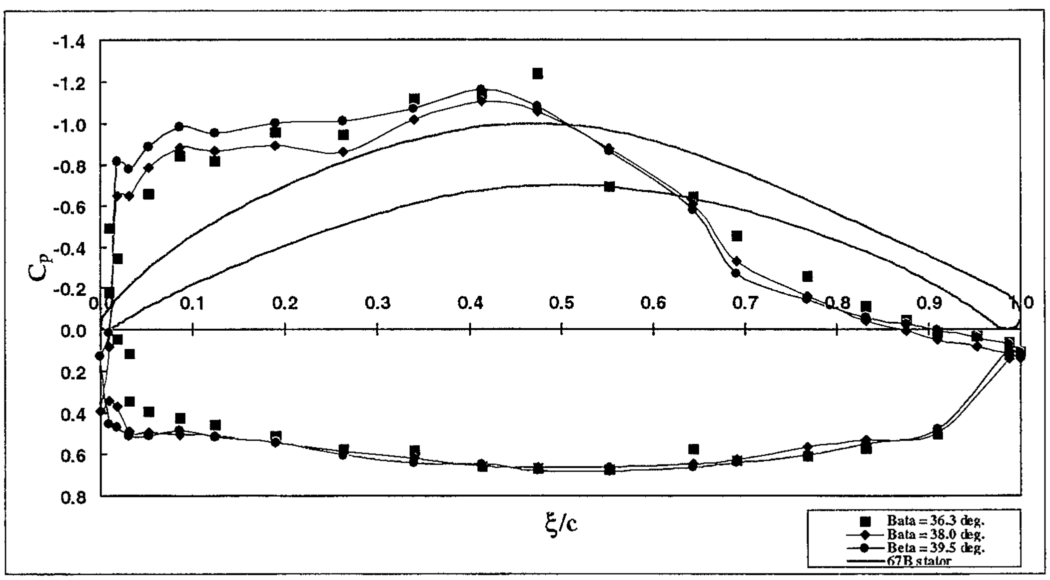

Figure 12. Comparison of C_p vs. ξ/c Plots for β = 36.3°, 38.0°, and 39.5°.

C. RAKE PROBE MEASUREMENTS

An upstream inlet survey across passage 3 was made using a 20-hole pneumatic rake probe. Total and static pressure measurements were obtained and plotted as C_p vs tunnel span, as shown in Figure 13 (1). An averaged inlet boundary layer thickness was found to be between 50.8-69.85 mm (2.0 - 2.75 in.) on the north wall of the tunnel, and about 76.2 mm (3 in.) on the south wall. Non-uniform boundary layers were attributed to wakes from the inlet guide vanes not being fully mixed out, particularly in the endwall regions. The C_p distribution in the center of the tunnel was constant over 40% of the span.

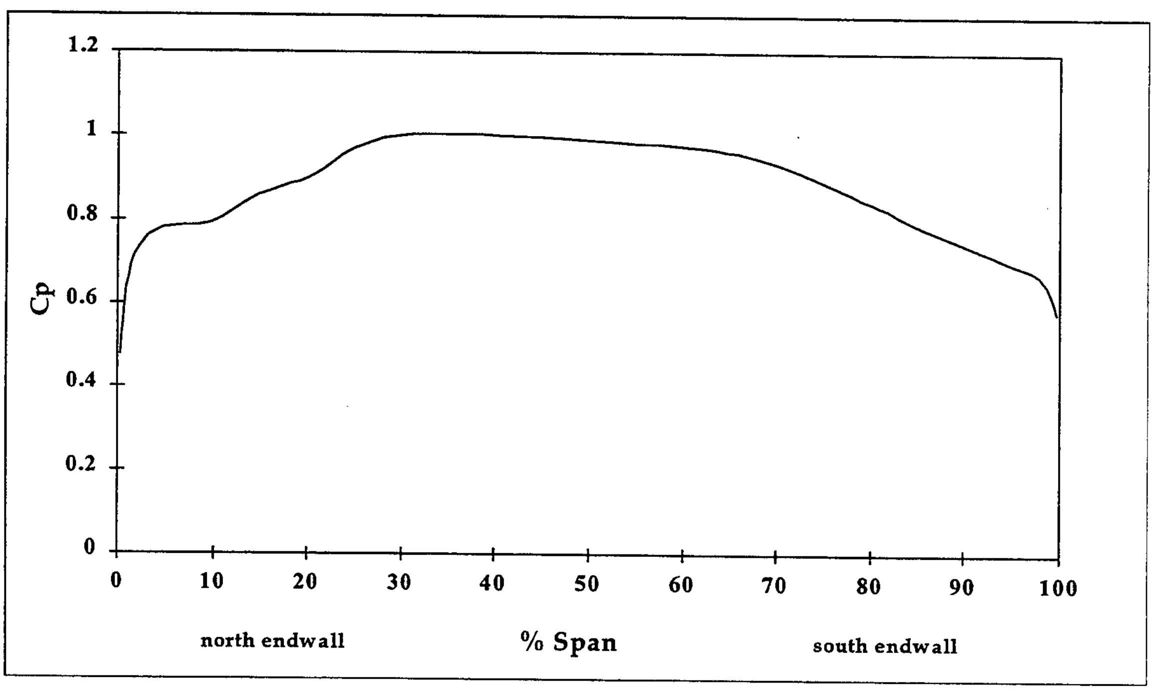

Figure 13. Upstream Spanwise C_p Distribution.

(1) Here, C_P is defined as the non-dimensional pressure, i.e., the local total pressure divided by the maximum total pressure measured by the rake probe.

D. LDV MEASUREMENTS

From blade surface flow visualization, it was shown that air flow was mostly symmetrical at the midspan. Separation of the boundary layer occurred at 0.5 C_{ac}. The C_p plot obtained from the fully instrumented blade showed that a possible separation occurred between 0.64 C_{ac} and 0.69 C_{ac} . LDV measurements at the midspan section were made for comparison with previous experimental data and to obtain a more detailed picture of the flow field characteristics around the blade.

1. Inlet Surveys

a. *Station 1*

Results showed nearly uniform velocity ratio's W/V_{ref} , U/V_{ref} , and V/V_{ref} as shown in Figure 14. The wave-like features of the velocity ratios were caused by upstream influence of the blade profiles since the disturbance repeated itself every blade spacing. Axial and tangential velocities gave an average inlet flow angle of 39.5° with a turbulence intensity of 2% for both the U and V velocity components. There was some indication of the unmixed inlet guide vane wakes in the turbulence intensity data for the tangential velocity (T_v) component which showed a three-per-blade spacing ripple. This could be due to wakes that had coupled together, however, this effect was not repeatably measured. The Reynolds-stress correlation coefficient remained at a constant value of 0.1, indicating a random or uncorrelated flow.

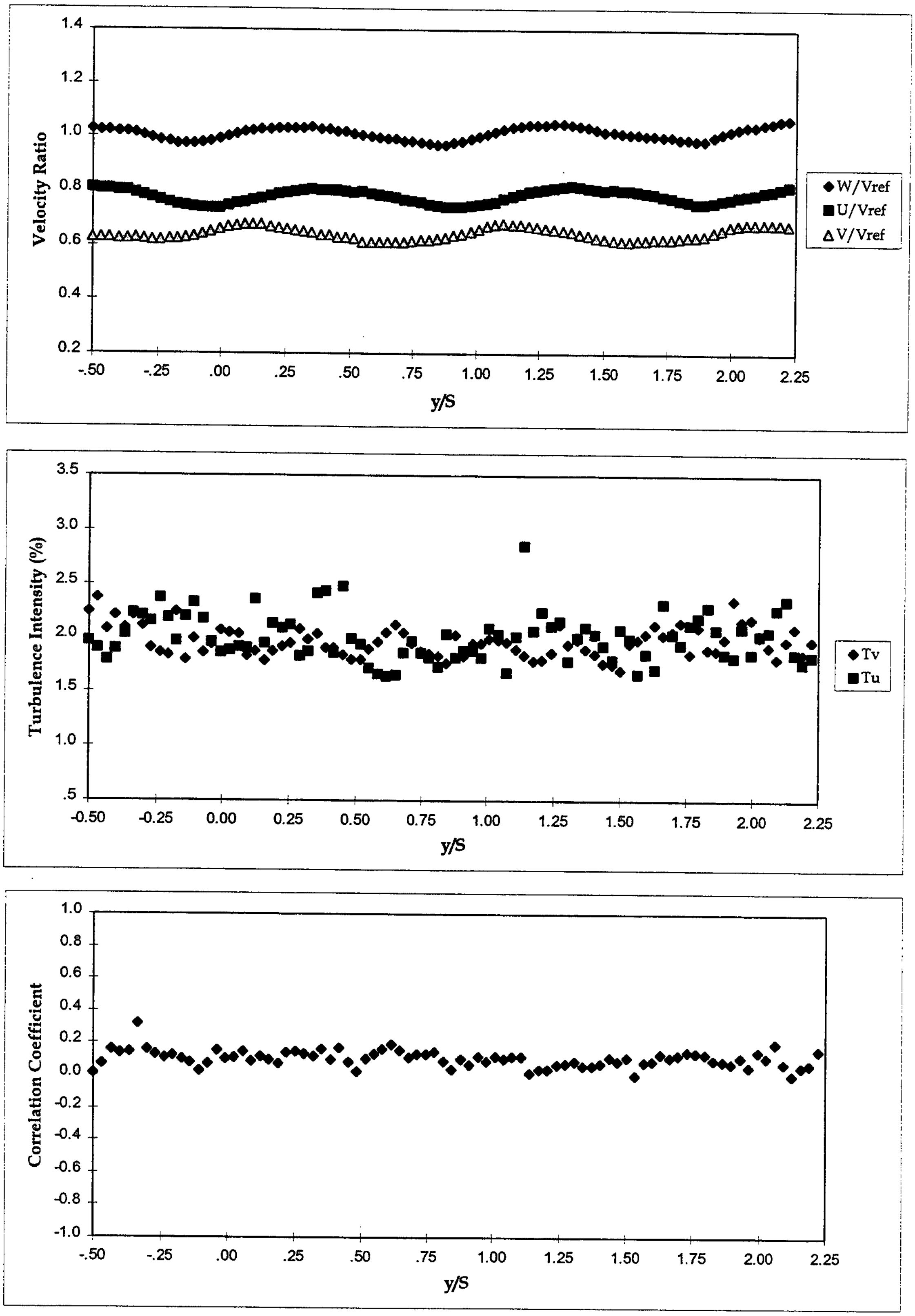

Figure 14. Inlet LDV Survey at Station 1.

It was found by LDV measurements that inserting the trip strip caused the inlet-flow angle (β_1) to changed from an average 38.0° to 39.5°. Since the inlet- flow angle and side-wall angle were not the same (1.5° difference), there was most likely a mild secondary flow entering the test section as shown in Figure 15. Repeatability tests were performed at this station with good results on the mean flow quantities.

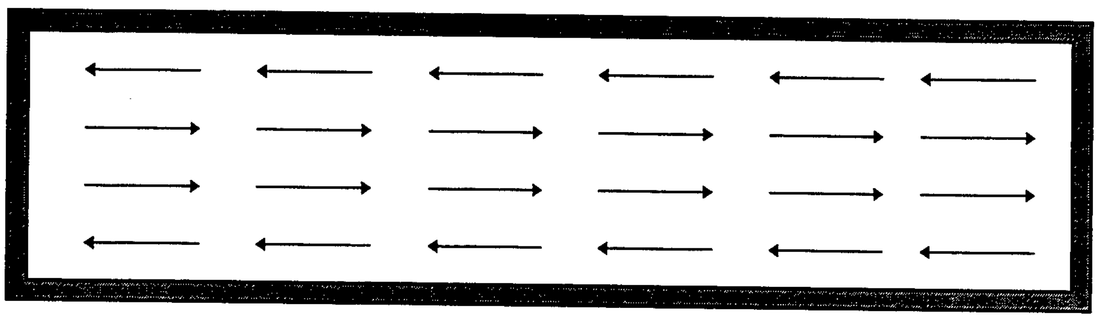

Figure 15. Possible Secondary Airflow Pattern.

b. *Station 3*

The survey results at station 3 are shown in Figure 16. Velocity ratio's W/V_{ref}, and U/V_{ref} decreased toward the leading edge of each blade. This was a result of potential effect of the blades on the approaching flow. The V velocity component was actually accelerated around the leading edge, thus the increase in V/V_{ref} was seen as the flow approached the blade. Turbulence intensity for both U and V velocity components stayed at 2.0% with a slight increase to 2.5 % on the suction side of the leading edge; while the correlation coefficient remained at 0.1.

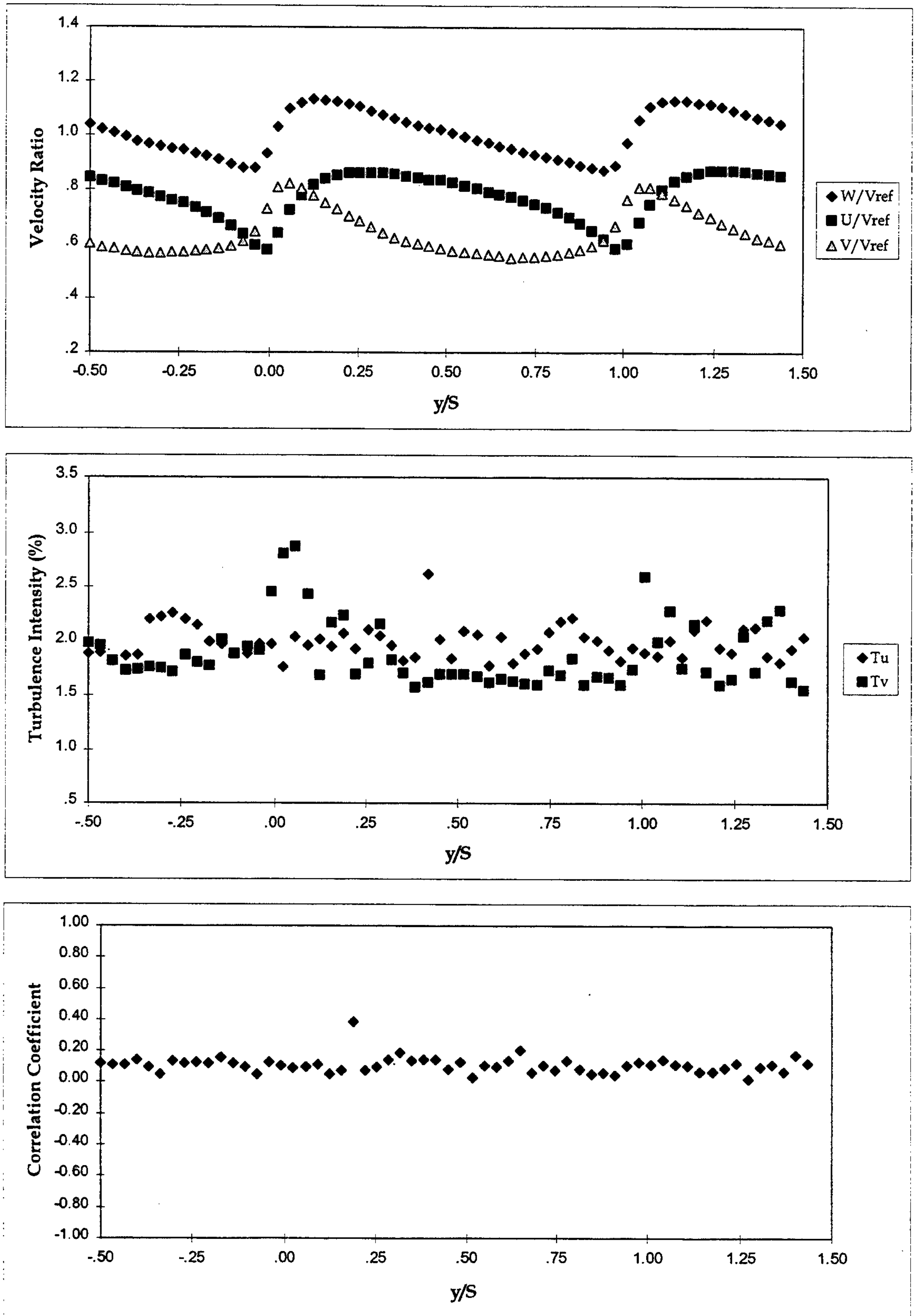

Figure 16. Inlet LDV Survey at Station 3.

2. Boundary Layer Surveys

Boundary layer surveys were performed at stations 6, 7, 8, and 9 on the suction side of blade #3. A test for periodicity was performed at station 8 on blade #4. Boundary layer data are presented in terms of the non-dimensional distance (d/c) perpendicular to the blade surface, where c is the blade chord length. The distance between each data point taken was 0.5 mm perpendicular to the surface of the blade for all stations. Comparison with previous results are discussed.

a. *Station 6*

The results obtained at station 6 (0.25 C_{ac}), are shown in Figure 17. Thirty eight data points were taken perpendicular to the blade surface. Results showed that the flow was turbulent and attached to the blade. Acceleration of the flow to 1.3 times the inlet reference velocity was measured. The second measured point (at a d/c of 0.008) was 2% higher than the first point, which indicated that the edge of the boundary layer was approximately at that distance from the blade surface. As shown in Figure 17, W/V_{ref} , U/V_{ref} , and V/V_{ref} gradually decrease in magnitude as distance from the blade increased and the pressure side of the passage was approached. Turbulence intensities remained relatively constant at 2.0 % over most of the survey. The correlation coefficient was 0.1. Previous experimental LDV surveys at β_1=38.0° (off-design) at 640,000 Re, showed similar results [Ref. 4].

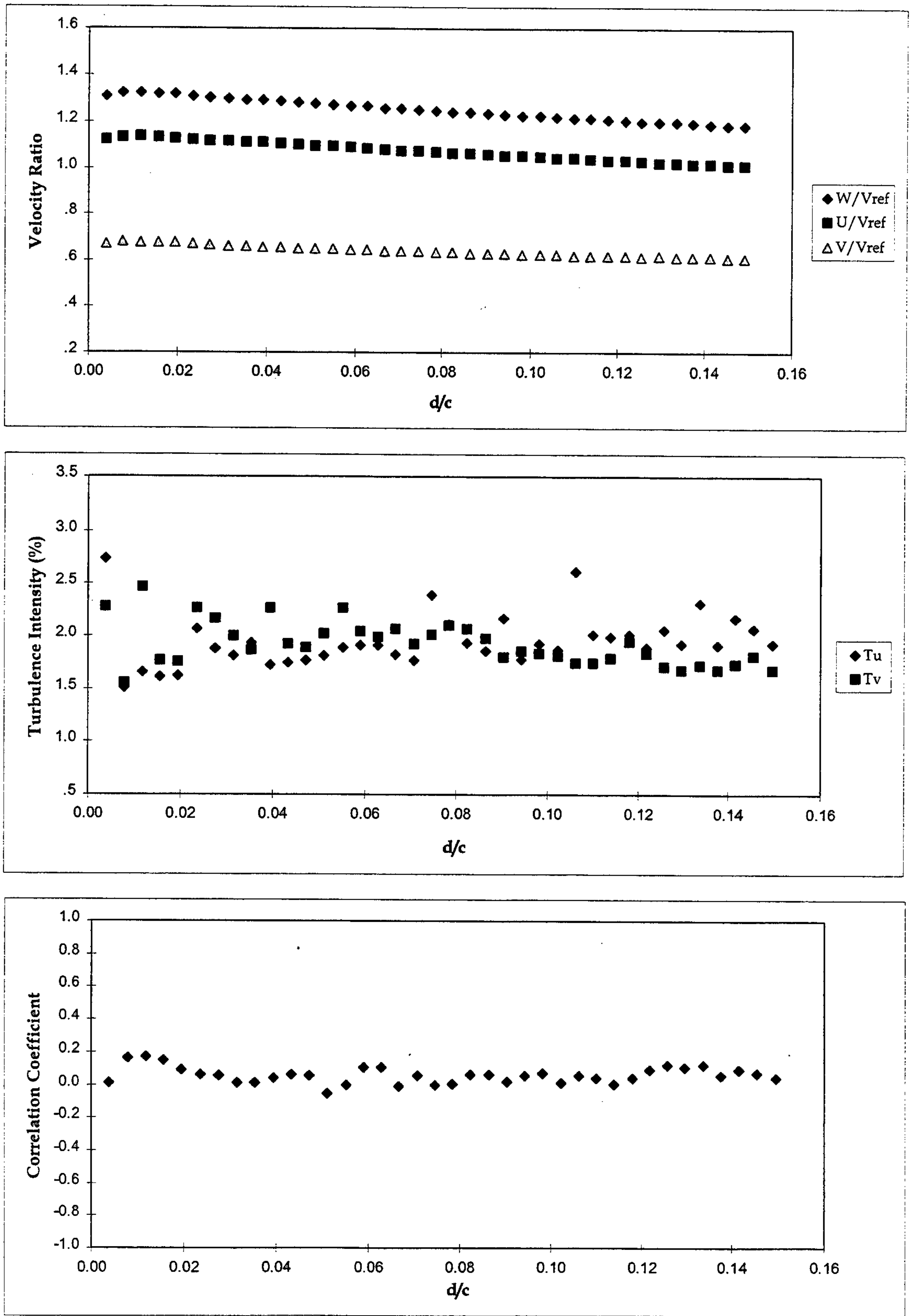

Figure 17. Boundary Layer LDV Survey at Station 6.

b. ***Station 7***

Station 7 (0.50 C_{ac}), was surveyed by collecting 40 data points perpendicular to the blade surface. Results are shown in Figure 18. The initial increase in W/V_{ref} , U/V_{ref} , and V/V_{ref} was within the boundary layer, where the thickness was measured at 0.02 d/c (2.54 mm out from the blade surface). The maximum total velocity ratio at the edge of the boundary layer was 1.1. Turbulence intensity for the U velocity reached a maximum of 18.0% at the surface of the blade and decreased to 2% at the outer edge of the boundary layer. Turbulence intensity for the V velocity component remained constant at 2% throughout the survey. The correlation coefficient first rose from a value of 0.0 to 0.1 at the surface of the blade and then decrease to a value of -0.41 at the outer edge of the boundary layer. It then gradually increased to a value of 0.0 at the end of the survey.

The survey showed that the boundary layer was most probably still attached, thus meaning that the separation point was further downstream than this station. This indicated that flow visualization results were contaminated due to gravitational effects. Comparing the velocity ratios obtained here with previous results showed that, for the 38.0° off-design incidence [Ref. 4], the results were similar. The turbulence intensities were also similar.

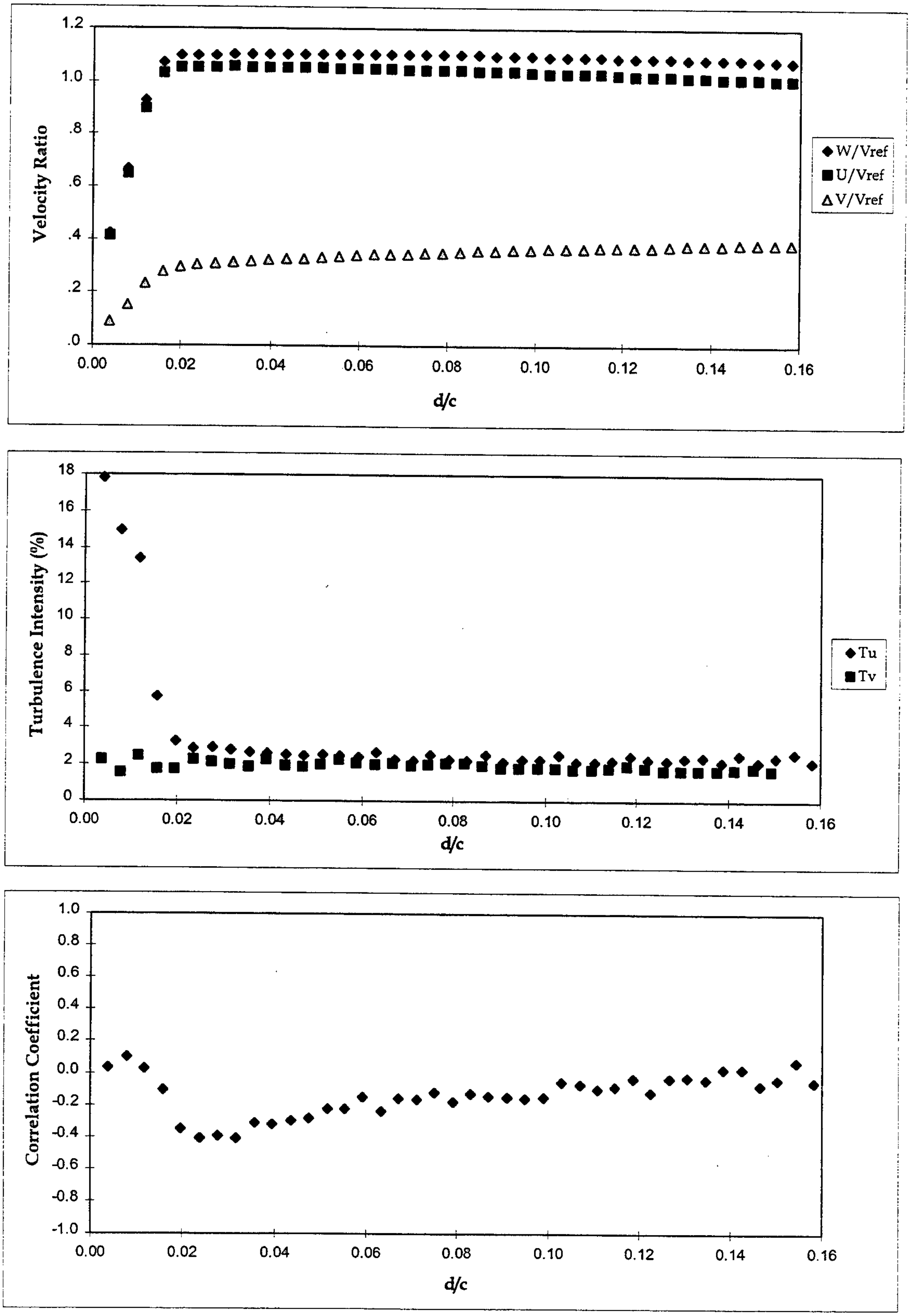

Figure 18. Boundary Layer LDV Survey at Station 7.

c. *Station 8*

Station 8, (0.75 C_{ac}) , was surveyed by collecting 43 data points perpendicular to the blade surface. Results shown in Figure 19 indicated that air-flow reversal was measured within the boundary layer from 0.0 to 0.06 d/c. The reverse flow velocity magnitude was approximately 10% of the reference velocity (V_{ref}). The V/V_{ref} ratio maintained a constant value of 0.0 until the value of 0.06 d/c was reached, at which time it increased gradually to a value of 0.3. This indicated that the V component velocity vector was always in the positive direction, i.e., diverging away from the blade surface.

The axial turbulence intensity (T_u) survey followed a Gaussian distribution. Initially it started at 5%, climbed to 30% at 0.085 d/c, and then dropped back down to 5%. The maximum turbulence corresponded to the maximum shear gradient in the axial velocity distribution. Tangential turbulence intensity T_v, only ranged from 5-9%. The correlation coefficient ranged from 0.1 to -0.1 throughout the survey.

A periodicity test was done at station 8 on blade #4 to see how well data matched with those at station 8 on blade #3. Results matched exceptionally well with no significant differences, as can been seen in Figure 20. Periodicity was also confirmed with the flow visualization pictures, (Fig. 10).

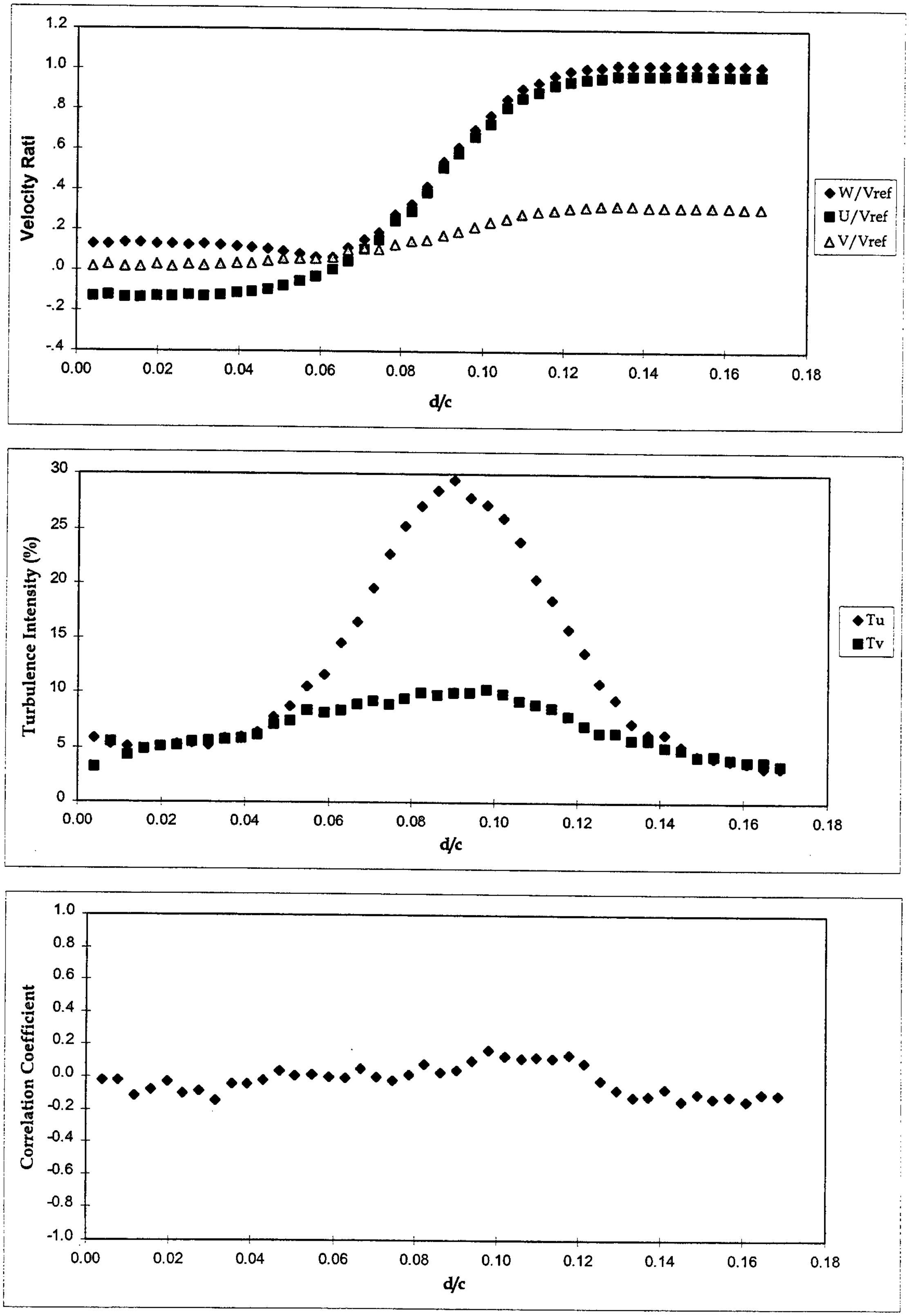

Figure 19. Boundary Layer LDV Survey at Station 8.

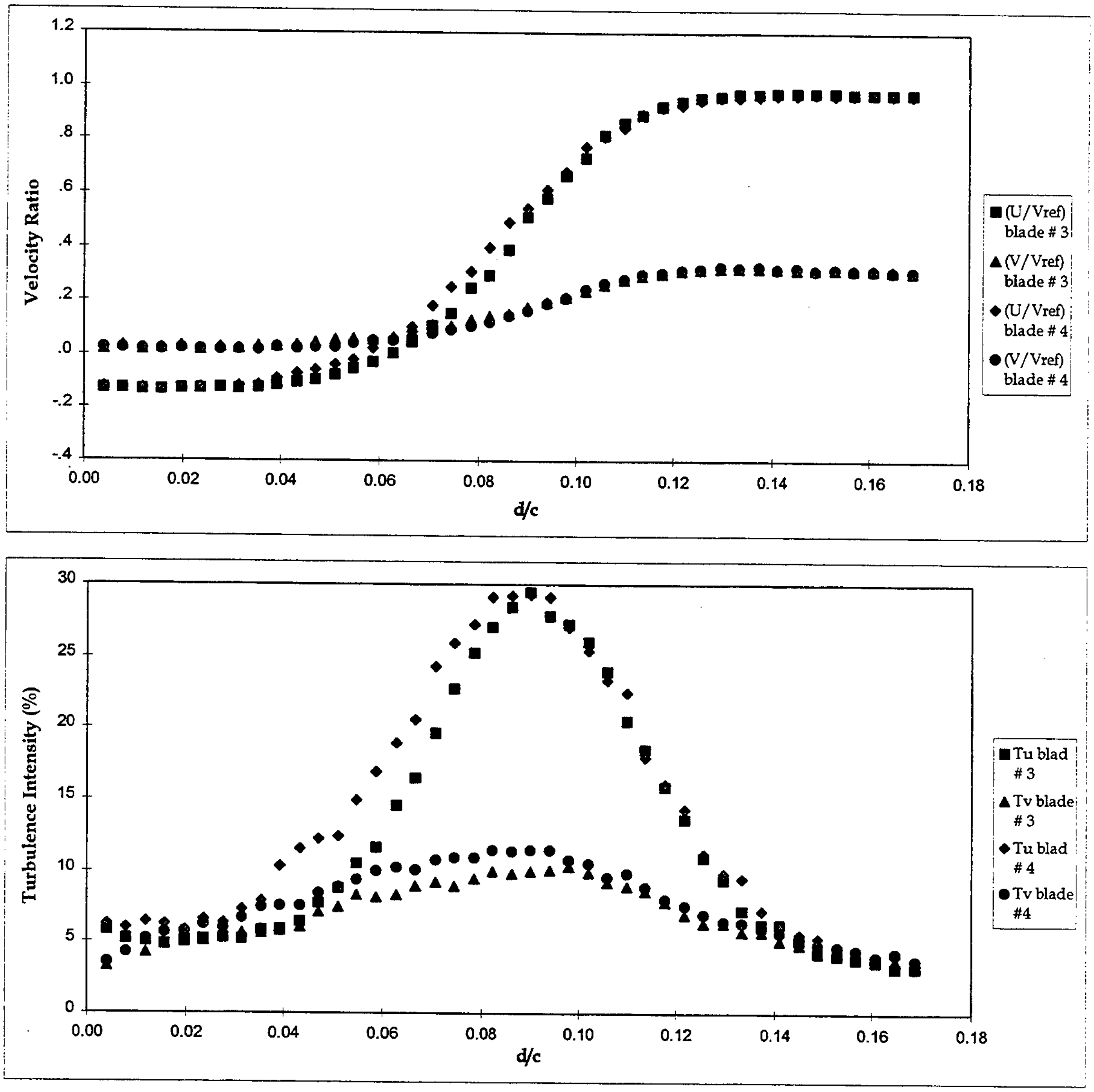

Figure 20. Comparison of Blades 3 and 4 Periodicity at Station 8.

d. *Station 9*

Station 9 (0.95 C_{ac}) , was surveyed by collecting 58 data points perpendicular to the blade surface. Results given in Figure 21, showed that flow reversal appeared within the boundary layer from the blade surface to a distance of 0.1 d/c. This can be seen in the distribution of the U/V_{ref} velocity ratio. From 0.1 d/c, U/V_{ref} increased to a maximum value of 1.0 at the outer edge of the boundary layer. V/Vref velocity ratio started out with a positive value of 0.1 and gradually decreased to a value of -0.1. This indicated that the flow direction was first positive (to the right of the vertical) and then eventually became negative (to the left of vertical).

Turbulence intensity T_u ranged from 5% to 30%, while turbulence intensity T_v ranged from 5% to 20%. The correlation coefficient began with a value of 0.0 and gradually climbed to 0.3 at 0.125 d/c and then gradually decreased back to 0.0.

Comparing the current study to the off-design case at β_1=38.0° [Ref. 4], little difference was found in the results. No simularity in data was evident when compared to the on-design case, at β_1=36.3° [Ref. 3].

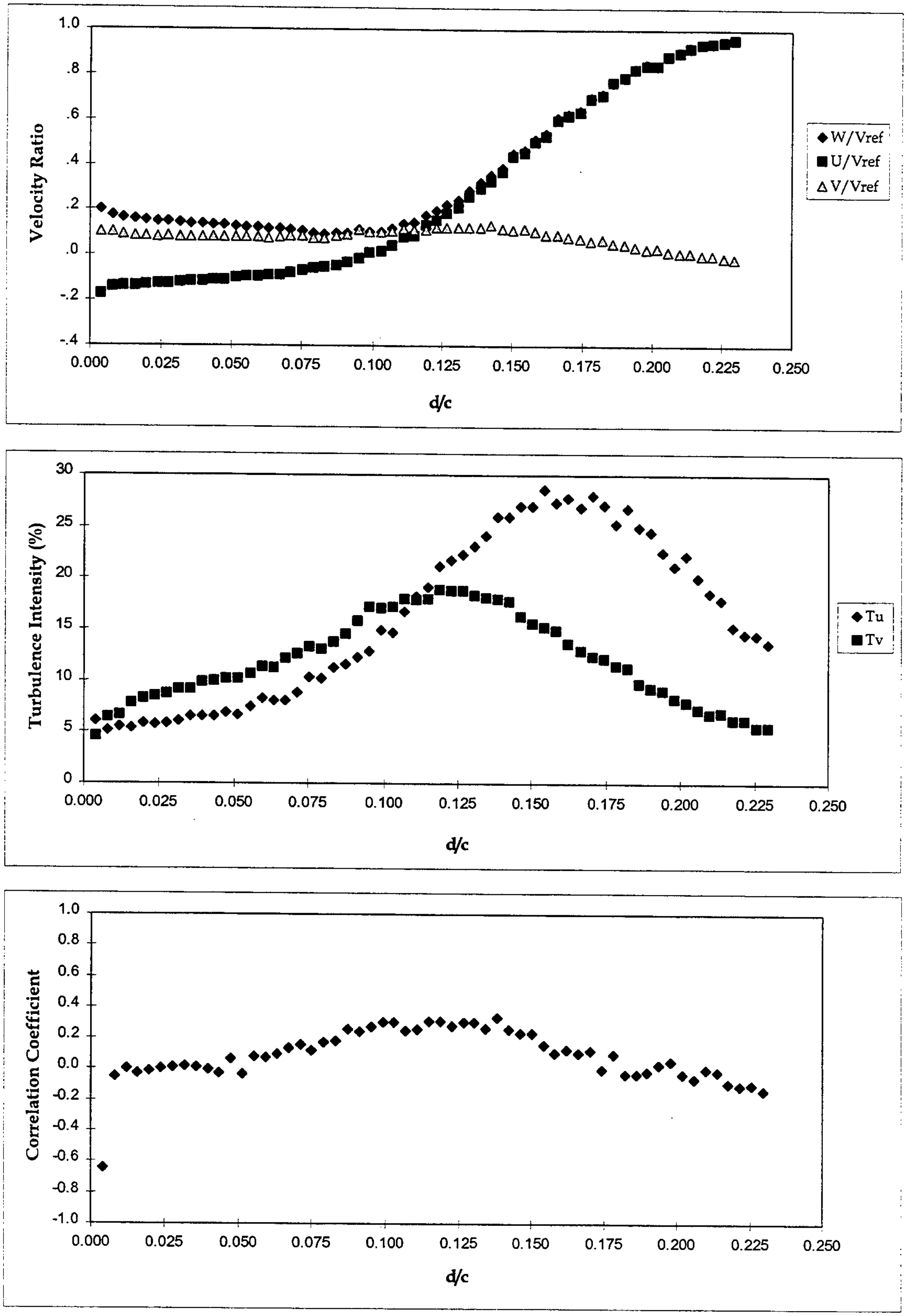

Figure 21. Boundary Layer LDV Survey at Station 9.

3. Wake Surveys

Wake surveys were performed at stations 11 and 13 over two blade passages as shown in Figures 22 and 23 respectively. Both had similar results and therefore only station 13 will be discussed.

a. *Station 13*

Station 13 was surveyed across two passages collecting 52 data points. The velocity profiles indicate a minimum at the trailing edge of each blade, noted by the deficit in the axial velocity distribution. In the freestream region, the velocity ratios indicated a slight decrease in magnitude on the suction side of the blade, then increased slightly as they approached the pressure side of the blade. The average exit angle was calculated to be 9.5° from the axial direction.

The axial turbulence intensity showed two peaks at the trailing edge of the blades, with a maximum value of 28%. Wake tangential velocity also had two peaks with a maximum value of 20%. The correlation coefficient varied from 0.4 to -0.4. The wake thickness was approximately 3.3% thicker for the current study when compared to the previous study [Ref. 4]. Comparing the results to the on-design [Ref. 3] case showed that the velocity ratios for the on-design case were shifted approximately 7.2 mm to the left, i.e., exit flow was turned more through the passage. Average exit flow angle was approximately 1.0° compared to 9.5° for the current study. Furthermore, wake thickness was approximately 14% less than that of the current study.

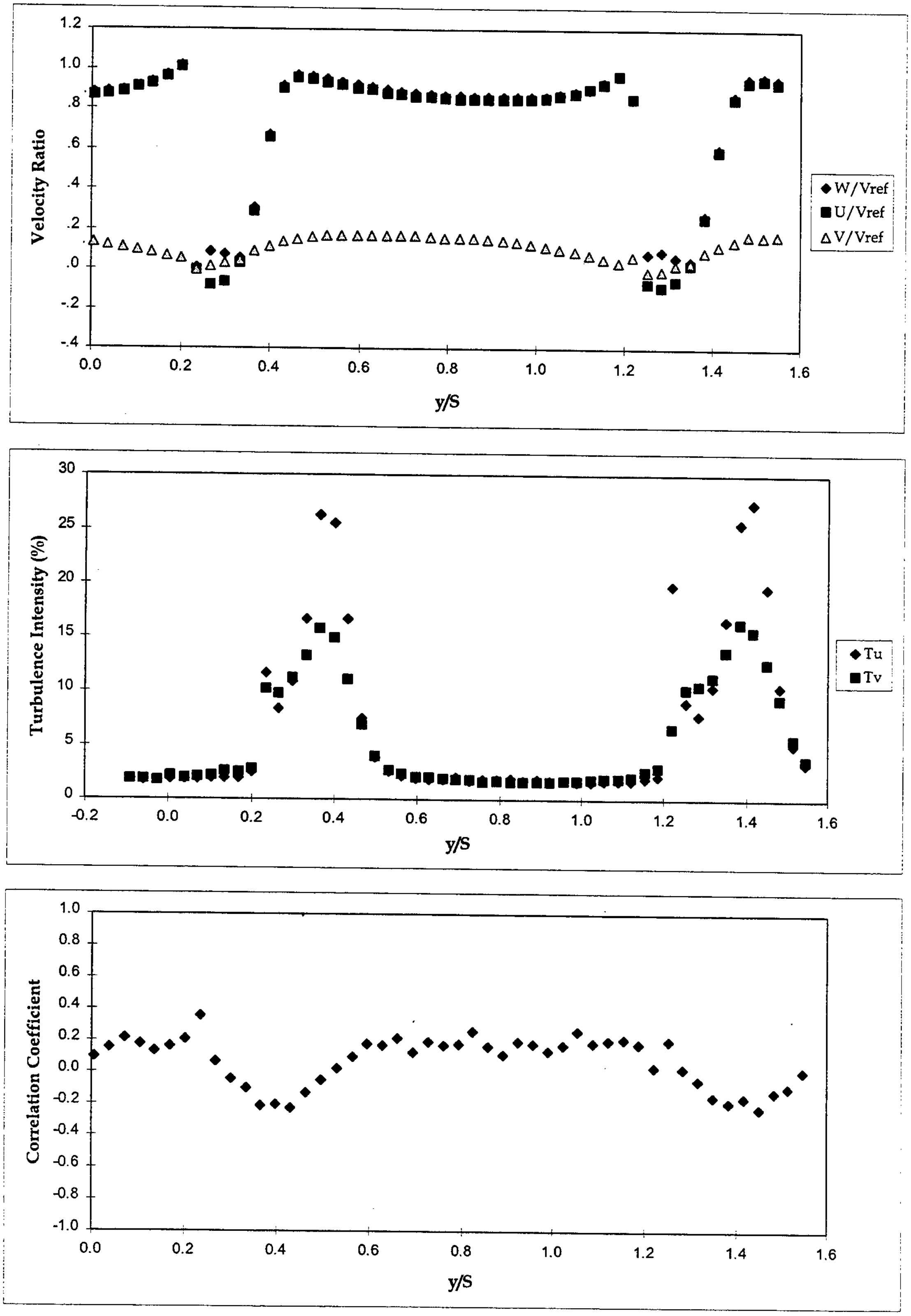

Figure 22. Wake LDV Survey at Station 11.

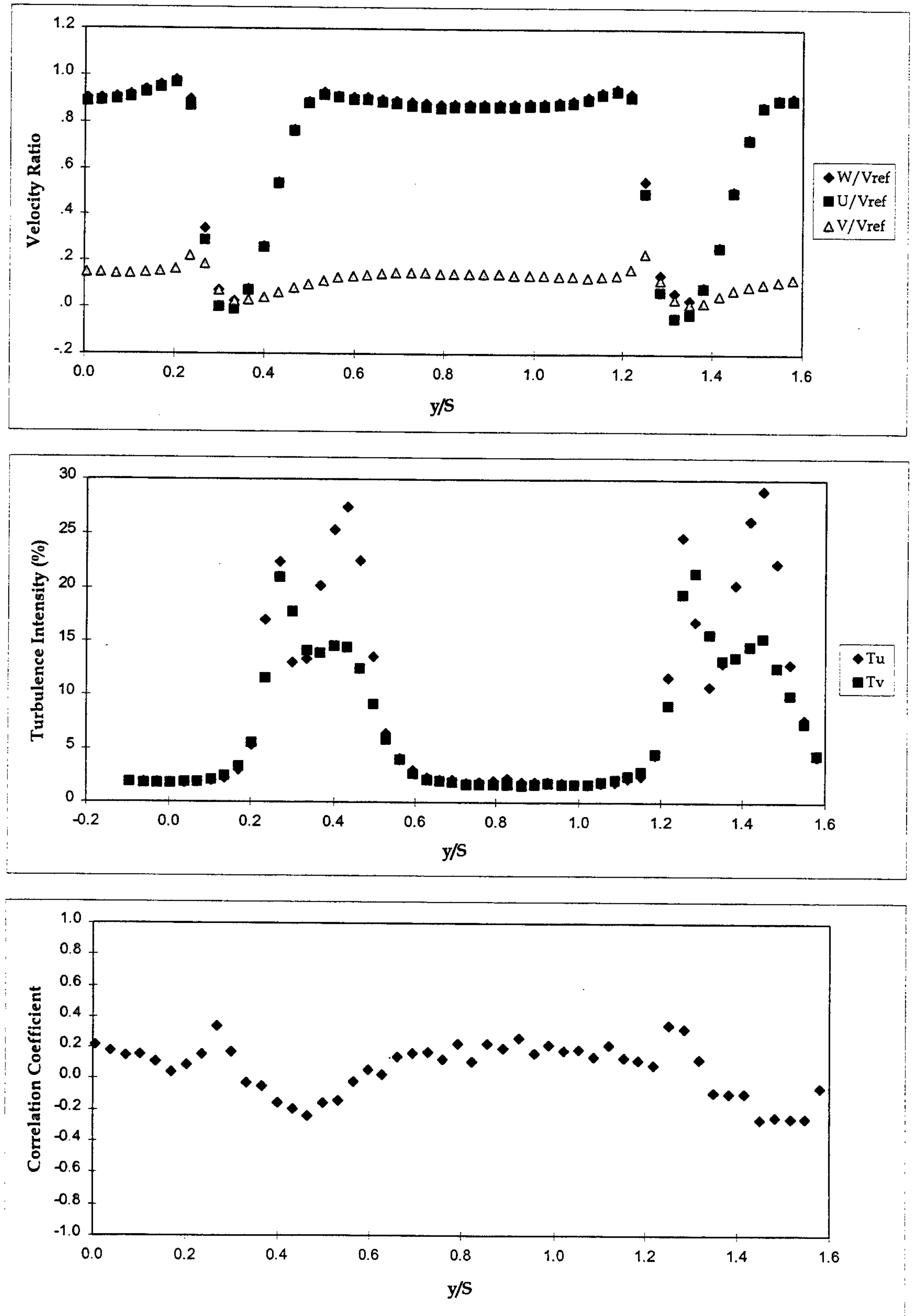

Figure 23. Wake LDV Survey at Station 13.

V. COMPUTATIONAL FLUID DYNAMIC (CFD) ANALYSIS

A. PURPOSE

The purpose of the numerical analysis was to obtain a solution that could be validated against experimental data obtained at an off-design incidence angle of 39.5°. Specifically, coefficient of pressures, flow reversal, and vortex locations could be compared. By validating the CFD solution with the experimental data, confidence is gained in the use of the code to arrive at designs that give improved blade performance.

B. NUMERICAL PROCEDURE

Computational fluid dynamic (CFD) analysis was performed using the Rotor Viscous Code 3-D (RVC3D - version 920318) developed by Dr. Roderick Chima of NASA Lewis Research Center [Ref. 11]. RVC3D is a computer code for analysis of three-dimensional viscous flow in turbomachinery. The code solved the thin-layer Navier-Stokes equations with an explicit finite-difference technique. Turbulence effects were modeled using a 3-D adaptation of the Baldwin-Lomax turbulence model. The equations were discretized using second-order finite-differences and were solved using a four-stage Runge-Kutta scheme.

A 3-D grid was generated around a single blade for half its span. A constant Courant number (CFL) of 5.0 was used throughout all the calculations. Grid generation and RVC3D inputs for numerical analysis can be found in Appendix E.

The C_P distribution from the inlet rake probe survey was used to calculate the inlet boundary layer thickness on the endwall. The test section Mach number was .22 at an inlet air angle β_1=39.5°. Angle of incidence was changed by changing the parameter 'prat' (static pressure of hub exit to inlet reference total pressure ($P_{hub\ exit} / P_o$)). Prat was calculated from rake probe measurements to be 0.9729 for a inlet angle of 39.5°.

The parameter "jedge" is defined as the last j-index (away from the airfoil) searched for the turbulent length scale. For the Balwin-Lomax turbulent model, "jedge" should be a grid line slightly bigger than the largest expected blade boundary layer. Initially this was set to the maximum of 49, which was much bigger than the boundary layer thickness indicated by the experimental data.

The "kedge" was the maximum grid surface (away from the endwall) to which the flowfield was searched for the turbulent length scale. The "jedge" and "kedge" parameters were relaxed from an inital value of 49 and 70 to a value of 30 and 50 respectively. One other parameter varied was "cmutm", the value of (eddy viscosity)/ (laminar viscosity) at which transition from laminar to turbulent is assumed to occur. Typically a value of 14 is normally used for natural transition and a value of 0.0 is used to simulate fully turbulent flow. The number was reduced to 10 because the flow was turbulent from close to the leading edge. Appendix F contains the output for the inlet and exit conditions that span in the K direction.

C. GRID GENERATION

A two-dimensional grid was first computed using a modified version of the FORTRAN code GRAPE (Grids About Airfoils using Poisson's Equations). Reference Hansen [Ref. 3] for code inputs. The grid size was 340 x 49. Grid coordinates were generated based on manufacturing dimensions. Next, a three-dimensional grid was built using a FORTRAN program called STACK, which took the two dimensional C-type grid and extended it outward in the z-direction for 70 grid points. The final grid ended up being a 340 x 49 x 70, which consisted of approximately 1.2 million grid points. Figure 24 shows the final grid.

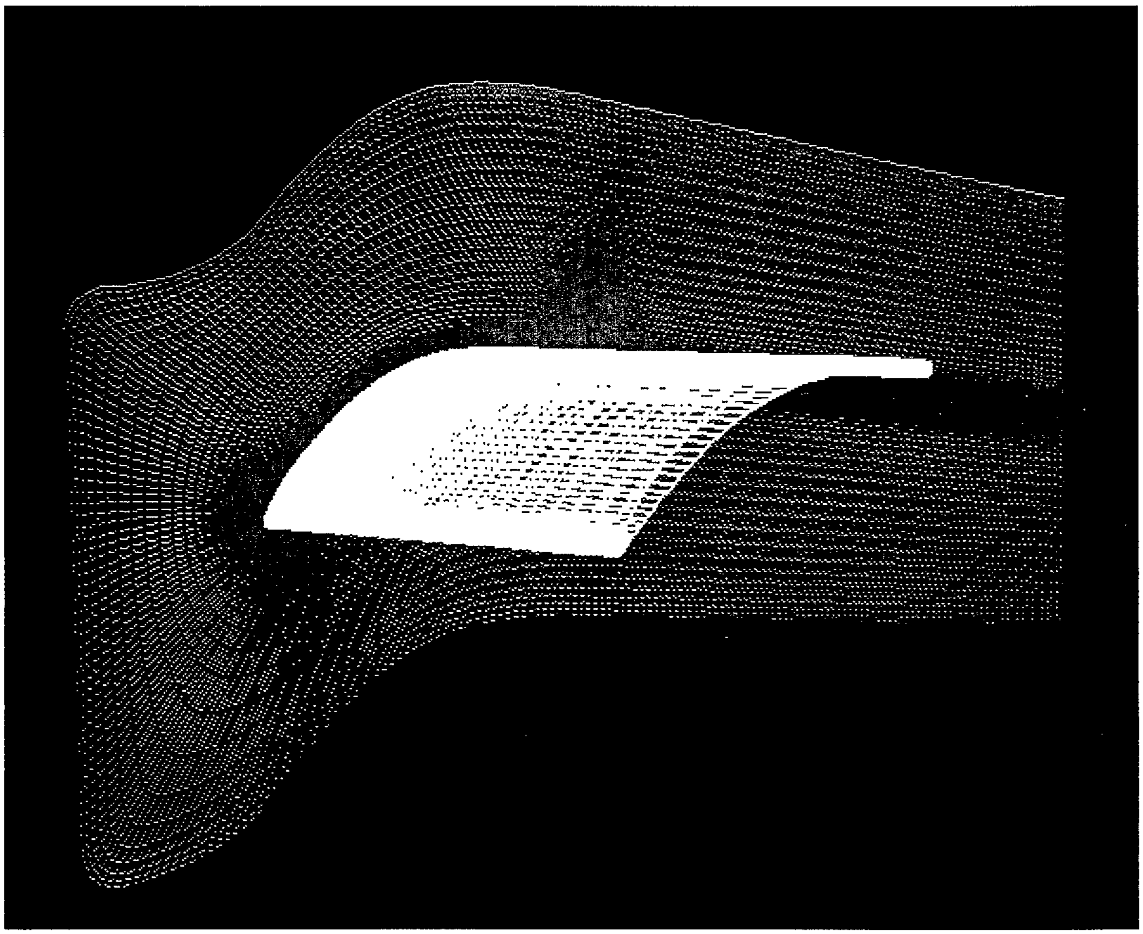

Figure 24. Three Dimensional C-type Grid of Half the Blade Span.

D. RESULTS AND DISCUSSION

1. Density Residual History

Figure 25 shows the density residuals up to seven thousand iterations. The residuals started out at a approximately 5.0 x 10^{-5} and decreased by three orders of magnitude in 7000 iterations. It took approximately 30 seconds per iteration on the CRAY J90 at NPS.

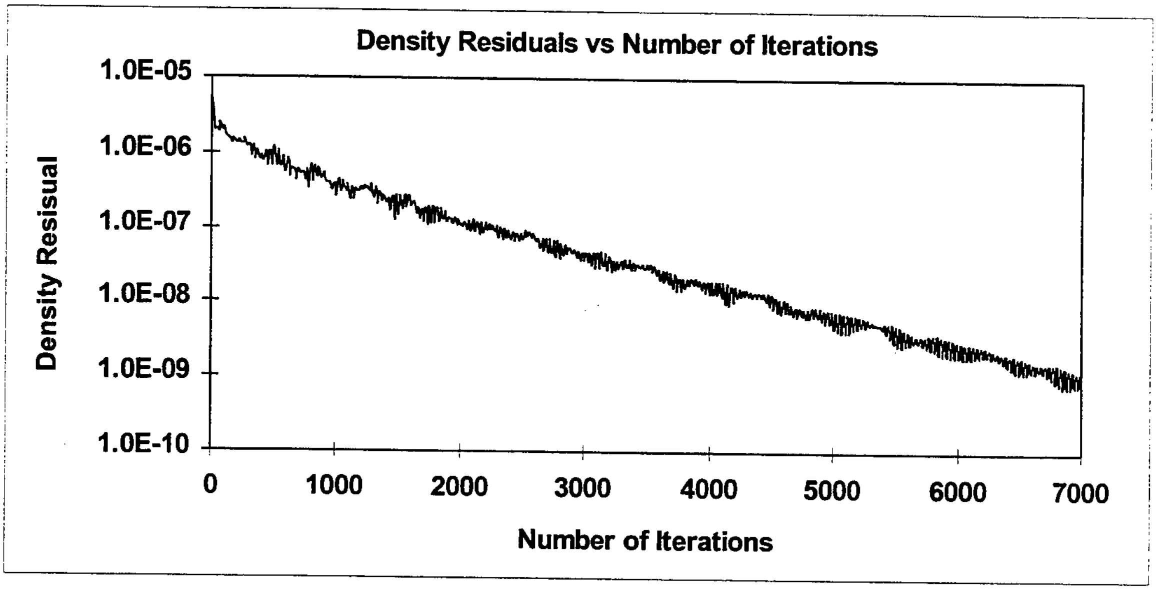

Figure 25. Convergence History.

2. FAST Flow Analysis

CFD flow visualization results showed good correlation with experimental studies. Figure 26 shows particle traces that indicated a vortex at approximately the same location as that of the experimental flow visualization. The red particle traces represent flow that is forced from the endwall towards the midspan of the blade. As can be seen with the yellow lines, some reverse flow over most of the blade and vortex formation near the endwall corner occured.

occured. CFD analysis did not pick up any reverse flow directly at the midspan, nor any separation bubble near the leading edge.

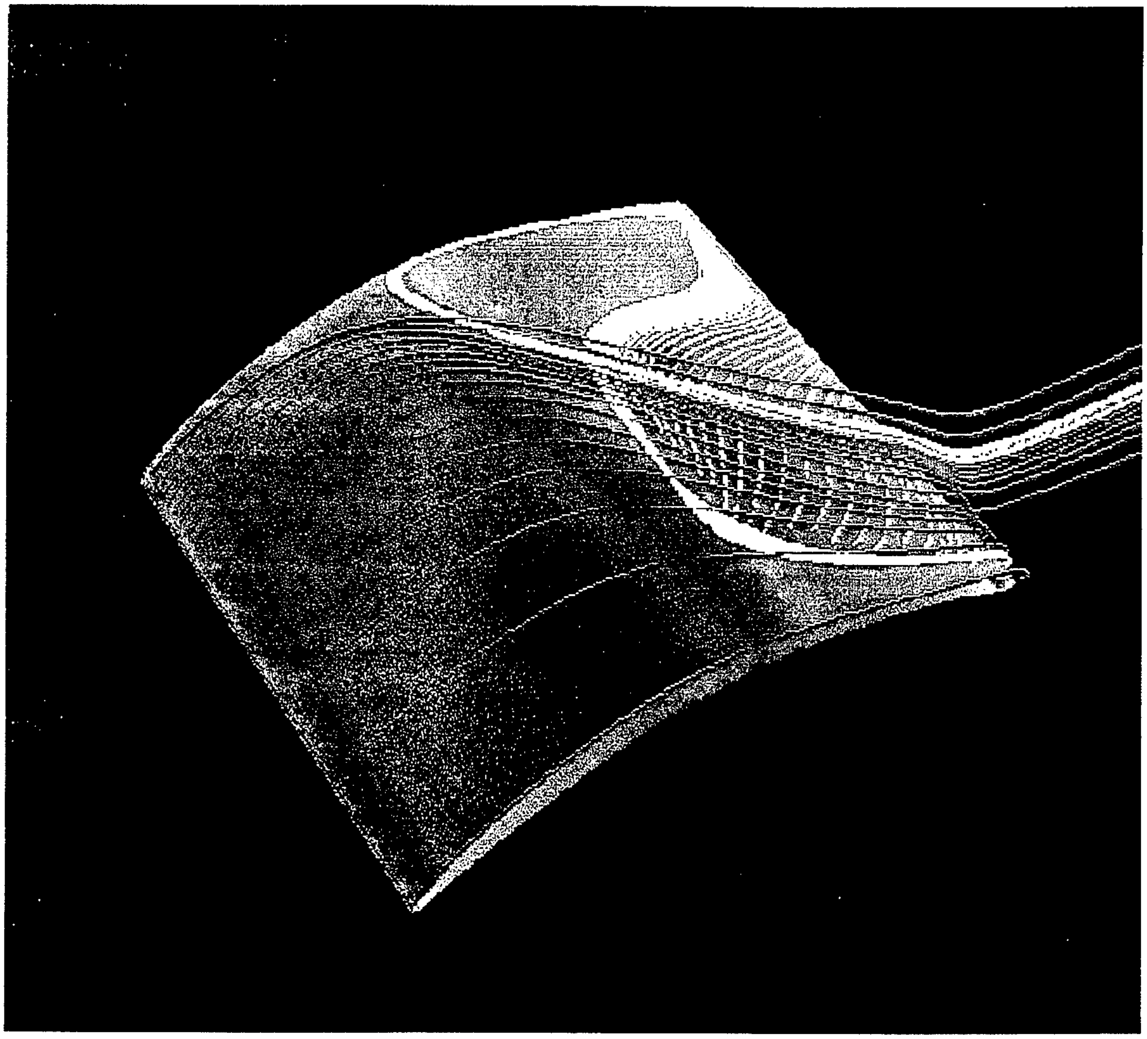

Figure 26. Particle Traces of the Flow Field over the Suction Surface.

3. Coefficient Of Pressure Distribution

Results for CFD vs. Experimental C_p distributions are shown in Fig. 27. There was an immediate decrease in pressure around the leading edge (suction side) of approximately -0.7 which sharply increased to -0.3 as predicted by the code. The solution was closely inspected with FAST, but no indication of a separation bubble was found, at the leading edge. The prediction for the pressure side of the blade matched up well with the experimental data. For the suction side of the blade, the shape of the predicted C_p profile seemed to agree in the axial direction but the magnitude was lower. The most noticeable difference was that the diffusion rate for the CFD analysis from approximately 0.45 to 0.7 ξ/c was less than was measured. This could explain why there was no boundary layer separation predicted at the midspan, which was the symmetry plane of the computational grid.

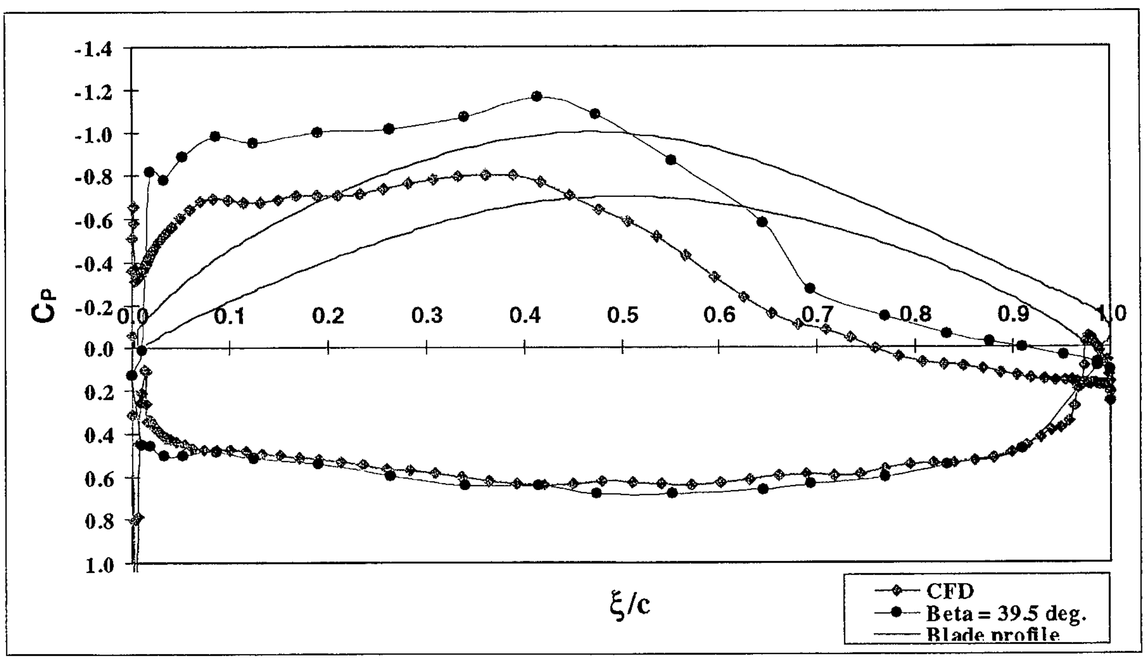

Figure 27. Predicted vs. Experimental C_p Distribution.

VI. CONCLUSION AND RECOMMENDATIONS

A. CONCLUSIONS

Compressor stator 67B cascade blading was successfully tested at an off-design inlet air angle of 39.5° in the Low-Speed Cascade Wind Tunnel. The experiments were conducted at a inlet test section Mach number of .22 and Reynolds number of 640,000. In each case, total plenum pressure, total plenum temperature, and ambient pressure were recorded to non-dimensionalize all data. The tunnel was successfully modified by inserting a fence into the south endwall boundary layer which made the flow more symmetrical about the midspan section. This made the midspan LDV measurements, of two velocity components in coincidence mode, more valid than previous studies.

Blade surface flow visualization was successfully performed using a titanium dioxide and kerosene mixture, and showed the symmetry of the flow at midpan of the blades. Periodicity was also observed with this technique.

Blade surface pressure measurements were obtained and compared to both previous experiments at lower inlet flow angles and numerical predictions of the three-dimensional flow through the blade row. A C_N vs β curve was generated using previous data from on-design incidence at $\beta 1=36.3°$, and off-design incidence at $\beta 1=38°$, and data from the current study. Results in Figure 28 showed that the blade was still working $\beta 1=39.5°$, even though boundary layer separation had occurred.

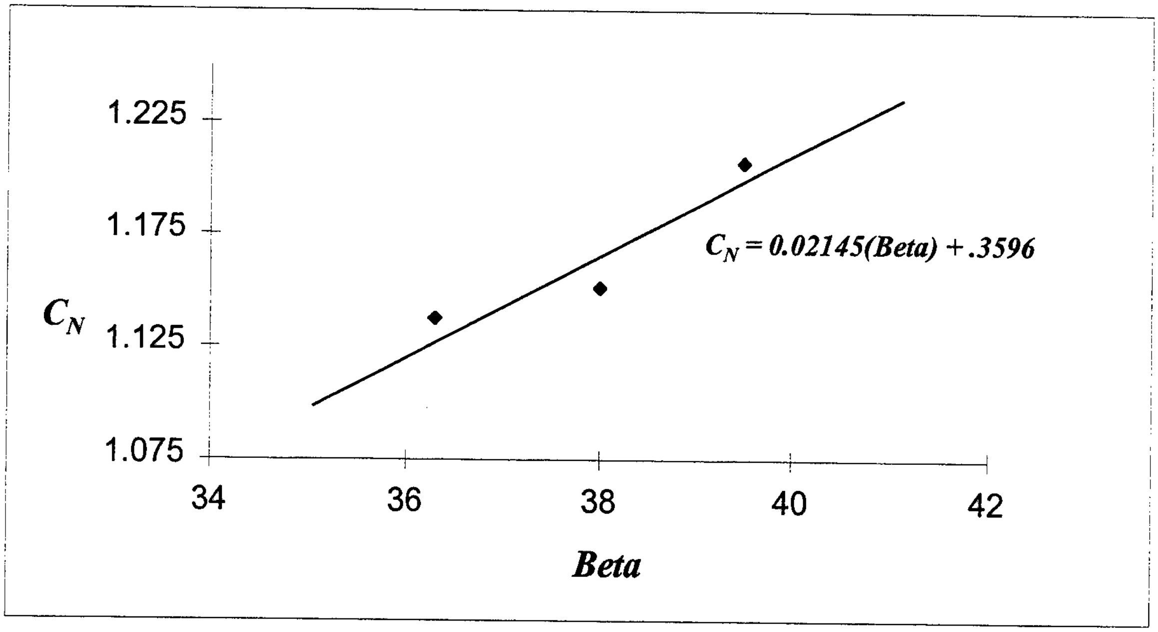

Figure 28. C_N vs. Beta Curve.

LDV surveys were completed at 8 different stations which characterized the flow in the inlet, the blade passage, and the wake area. Reverse flow was measured in the suction surface boundary layer aft of 75% axial chord. Reverse flow was also measured in the wake at 105 and 120% axial chord from the leading edge.

CFD analysis was performed and results were in reasonable agreement with experimental data. Vortex flow at the trailing edge of the blade and near the endwall was indicated by the solution. However, no indication of reverse flow was found at midspan.

B. RECOMMENDATIONS

Further LDV studies should be performed at and near the leading edge of the blade on the suction side to see if a separation bubble exists. Three-dimensional surveys should be performed in order to characterize the flow in endwall region. This will allow better mapping of the air flow to more thoroughly validate the CFD code.

Further CFD studies should be initiated to try and match the Cp distribution as close as possible by varying the input parameters. Then, and only then can the CFD code be fully validated by the experimental data.

APPENDIX A.

MIXING INSTUCTIONS FOR TITANIUM DIOXIDE & KEROSENE

STEPS

1. Put 6 Oz's of Pure Vegetable Oil in a one-quart plastic container.
2. Put about 1 tablespoon of Saturn yellow pigment in sifter and sift into container.
3. Mix well with hand stirrer/tongue depressor.
4. Put 2 scoops (little plastic cup) of TiO_2 into sifter and sift as much as you can into the container. Dump the big chunks back into TiO_2 can. Repeat this step 2 more times.

Note: It may take 10-15 minutes for each time of sifting. Mix the contents by hand before each repeat. Do not attempt to push the TiO_2 through the sifter.

5. Add 4 Oz's of Kerosene (more can be added to make mixture thinner)
6. Add 20 squirts of oil (SAE 30) from an oil can.
7. Put on magnetic mixer and mix for 10-15 minutes.

APPENDIX B.

TABLE OF SCANIVALVE PORTS
AND
CHANNEL ASSIGNMENTS

Scanivlave #1
Blade Pressure Measurements

1	Atmosphere	25	3 Suct. Side
2	Calibration	26	4 Suct. Side
3	Plenum Press	27	5 Suct. Side
4	18 Press Side	28	6 Suct. Side
5	17 Press Side	29	7 Suct. Side
6	16 Press Side	30	8 Suct. Side
7	15 Press Side	31	9 Suct. Side
8	14 Press Side	32	10 Suct. Side
9	13 Press Side	33	11 Suct. Side
10	12 Press Side	34	12 Suct. Side
11	11 Press Side	35	13 Suct. Side
12	10 Press Side	36	14 Suct. Side
13	9 Press Side	37	15 Suct. Side
14	8 Press Side	38	16 Suct. Side
15	7 Press Side	39	17 Suct. Side
16	6 Press Side	40	18 Suct. Side
17	5 Press Side	41	19 Suct. Side
18	4 Press Side	42	20 Suct. Side
19	3 Press Side	43	TE
20	2 Press Side	44	Blade 8, 1 Suct.
21	1 Press Side	45	Blade 8, 2 Suct.
22	LE	46	Blade 8, 3 Suct.
23	1 Suct. Side	47	Blade 8, 4 Suct.
24	2 Suct. Side	48	Blade 8, 5 Suct.

TABLE - B1

Scanivalve #2
Rake Probe Measurements

1	Atmosphere	25	Rake yaw
2	Calibration	26	Rake total
3	Plenum Press	27	Rake total
4	P Wall Static	28	Rake total
5	Not Used	29	Rake total
6	Not Used	30	Rake total
7	Not Used	31	Rake total
8	Not Used	32	Rake total
9	Not Used	33	Rake total
10	P Prandtl tot	34	Rake total
11	P Prandtl stat	35	Not Used
12	Atmosphere	36	Not Used
13	Calibration	37	Not Used
14	Plen. P (tot)	38	Not Used
15	Rake total	39	Not Used
16	Rake total	40	Not Used
17	Rake total	41	Not Used
18	Rake total	42	Not Used
19	Rake total	43	Not Used
20	Rake total	44	Not Used
21	Rake total	45	Not Used
22	Rake total	46	Not Used
23	Rake static	47	Not Used
24	Rake yaw	48	Not Used

TABLE - B2

APPENDIX C.

FIND (2-D) SOFTWARE INPUTS

<A> Color link: off
Traverse: TSI Model 9500 Processors: 2 Mode: Coincidence.
Date File: d:**\(filename) Data sample size: 1K Data Points

<I> I/O PORT AND PROCESSOR TYPE SELECTION
<P> PROCESSOR SETTINGS
<O> OPTICS CONFIGURATION
<E> EXPERIMENT DOCUMENTATION AND INPUTS
<H> HARDWARE DIAGNOSTICS
<F> DATA FILE MANAGEMENT
<T> AUTOMATIC TRAVERSE PARAMETERS
<R> REALTIME HISTOGRAM
<M> RETURN TO MAIN MENU

<F2> ACQUIRE DATA FOR (# OF) RAW DATA FILES
<F3> STORE PROGRAM DOCUMENTATION
****

This section shows what is under each sub-menu and the inputs

<I> I/O PORT AND PROCESSOR TYPE SELECTION

Color link: off
Traverse: TSI Model 9500 Processors: 2 Mode: Coincidence.
Date File: d:**\(filename) Data sample size: 1K Data Points

I/O Port Selections		LDV Processor Type	
Traverse Controller	= COM 2	First Processor	= 1990
Sony Position Encoder	= COM 1	Second Processor	= 1990
Printer Port	= LPT 1	Third Processor	= 1990
Processor I/O	= COM 1		
Color Link	= Off	Master Interface	= 1998A

Program Installation Settings

Computer Bus Type	= PCBUS	Graphic Type	= EGA
Monitor Type	= Color	Toggle Selection	= High light

DMA Chan: 1, Port Addr: 300H Com1-Com4 Addr: 3F8H;2F8H;3E8H;2E8H

<P> *PROCESSOR SETTINGS*

*********************************Interface / DMA Selection****************

Number of Processors:	2
Number of K-Data Points:	1 K
Data Sampling Method:	TBD-ON
Coincidence Window width (μs)	2.0 E5
DMA Timeout (seconds)	300
Acquisition Mode	Coincidence

*********************************Processor Selections**********************

		Processor 1	Processor 2
Number of Cycles:		8	8
Processor Type		1990	1990
Processor Mode		CONT.	CONT.
Filter Range	High limit:	50 Mhz	50 Mhz
	Low limit:	.3 Mhz	.3 Mhz
Timer Comparison		1	1
Gain		1	1

<O> *OPTICS CONFIGURATION*

Using Half Angle Calculation

	Green beam	Blue beam
Fringe Spacing (microns)	4.7569	4.5119
Frequency Shift	+5 Mhz	+5 Mhz
Half Angle	3.1	3.1
Focal Length (mm)	762	762
Beam Spacing (mm)	82.5	82.5
Wave length (nm)	514.5	488

APPENDIX D.

LDV SUMMARY AND REDUCED DATA

Station	Survey Name	Date Taken	Re # x 10^5	Survey Points	Patm (psi)	P_{Pl} " H_2O	T_{Pl} F	Vref (m/s)	Yaw-Pitch deg.
1	0205igvs	2/05/97	6.4	84	14.76	12.1	70	77.034	
1	0207igvs	2/07/97	6.4	84	14.76	12	70	76.724	
3	0301inl3	3/01/97	6.4	60	14.78	12	70	76.674	
6bl	0211bl63	2/11/97	6.4	40	14.76	11.9	65	76.051	Yaw 4° L
7bl	0211bl73	2/11/97	6.4	40	14.76	11.9	68	76.268	Yaw 4° L
8bl	0204bl8	2/04/97	6.4	47	14.75	12	69	76.677	Yaw 4° L
8bl	0207bl84	2/07/97	6.4	47	14.76	12	72	76869	Yaw 4° L
9bl	0218bl93	2/18/97	6.4	60	14.8	12.2	66.5	76.370	Yaw 4° L
11wk	0302wk11	3/02/97	6.4	50	14.78	12.3	67.5	77.417	
13wk	0302wk13	3/02/97	6.4	52	14.78	12.2	70	77.292	

Station 1 Inlet survey 0205igvs
Vref = 77.0344 m/s
Blade spacing (s) = 152.4 mm

x(mm)	y(mm)	y/s	W/Vref	U/Vref	V/Vref	Tu	Tv	Re Stres	Corr.
36.578	-76.200	-.500000	1.026475	.810958	.629284	2.235431	1.969092	.034346	.013149
36.576	-71.200	-.467192	1.024767	.810230	.627435	2.368838	1.903268	.189937	.070991
36.576	-66.200	-.434383	1.024554	.809213	.628400	2.079765	1.794213	.354126	.159919
36.578	-61.200	-.401575	1.021069	.806122	.626698	2.210942	1.894665	.340190	.136849
36.576	-56.200	-.368766	1.019414	.804089	.626615	2.088074	2.029255	.363449	.144542
36.576	-51.200	-.335958	1.012841	.795211	.627285	2.208706	2.231371	.942315	.322194
36.576	-46.200	-.303150	1.004851	.787782	.623799	2.113311	2.207089	.433164	.156495
36.576	-41.200	-.270341	.995244	.776736	.622248	1.906444	2.154117	.316459	.129854
36.576	-36.198	-.237520	.988910	.769120	.621609	1.861970	2.373634	.285422	.108826
36.576	-31.200	-.204724	.982814	.759045	.624318	1.833299	2.187337	.293819	.123470
36.576	-26.200	-.171916	.976912	.749823	.626197	2.235156	1.965043	.261190	.100209
36.576	-21.200	-.139108	.976397	.746951	.628820	1.795378	2.195797	.189944	.081191
36.576	-16.200	-.106299	.977130	.742594	.635088	1.991363	2.328797	.084533	.030717
36.576	-11.200	-.073491	.977985	.738052	.641665	1.858039	2.168508	.168486	.070466
36.576	-6.200	-.040682	.984752	.738627	.651280	1.932832	1.959527	.334054	.148629
36.576	-1.200	-.007874	.991372	.740507	.659142	2.061734	1.853566	.229140	.101039
36.576	3.800	.024934	1.001260	.746047	.667783	2.040185	1.879690	.241015	.105905
36.576	8.800	.057743	1.012094	.754678	.674384	2.035036	1.912183	.340049	.147255
36.576	13.800	.090551	1.019902	.761038	.678986	1.828333	1.905636	.180719	.087406
36.576	18.800	.123360	1.025448	.769425	.677885	1.870365	2.354391	.299599	.114648
36.576	23.800	.156168	1.028899	.774114	.677776	1.780501	1.947604	.191307	.092964
36.576	28.800	.188976	1.029185	.783741	.667063	1.873728	2.130739	.169418	.071508
36.576	33.800	.221785	1.032238	.791044	.663148	1.916462	2.083452	.320219	.135143
36.576	38.800	.254593	1.032976	.795558	.658884	1.950055	2.124517	.358578	.145850
36.576	43.800	.287402	1.034046	.801230	.653668	2.072839	1.828642	.301525	.134047
36.576	48.800	.320210	1.033633	.803436	.650298	1.978879	1.873638	.257700	.117123
36.576	53.800	.353018	1.034743	.807868	.646562	2.029040	2.414294	.453496	.155999
36.576	58.800	.385827	1.027606	.804766	.639003	1.898122	2.437285	.255952	.093231
36.576	63.800	.418635	1.027550	.806048	.637296	1.905489	1.863899	.356707	.169244
36.576	68.800	.451444	1.021105	.803651	.629921	1.833973	2.474853	.222942	.082772
36.576	73.800	.484252	1.018137	.801673	.627634	1.792589	1.993051	.045354	.021392
36.576	78.800	.517060	1.010864	.796201	.622824	1.788300	1.937843	.206588	.100456
36.576	83.800	.549869	1.005757	.798387	.611658	1.896482	1.716704	.245620	.127131
36.576	88.800	.582677	1.000968	.792398	.611590	1.960686	1.660364	.306887	.158854
36.576	93.800	.615486	.995816	.786890	.610290	2.045835	1.644792	.377188	.188889
36.576	98.800	.648294	.991264	.780837	.610653	2.115896	1.648440	.320054	.154627
36.576	103.800	.681102	.991464	.778857	.613500	2.048480	1.858874	.242873	.107480
36.576	108.800	.713911	.984175	.770142	.612767	1.947927	1.972771	.289570	.126979
36.576	113.800	.746719	.984104	.765977	.617851	1.865568	1.858046	.271535	.132005
36.576	118.800	.779528	.979712	.758716	.619828	1.848201	1.811851	.294544	.148221
36.576	123.800	.812336	.977023	.753263	.622229	1.821775	1.725110	.166516	.089284
36.576	128.800	.845144	.972492	.746276	.623549	1.756255	2.031621	.084194	.039763
36.576	133.800	.877953	.972112	.741556	.628567	2.021511	1.814485	.222946	.102423
36.576	138.800	.910761	.977378	.741012	.637314	1.829536	1.885812	.135546	.066203
36.576	143.800	.943570	.982333	.742963	.642639	1.943598	1.877559	.257272	.118802
36.576	148.800	.976378	.992331	.747578	.652571	1.950243	1.814584	.184453	.087832
36.576	153.800	1.009186	1.000988	.751081	.661706	1.992994	2.084069	.277490	.112580
36.576	158.800	1.041995	1.012277	.757795	.671157	1.978906	2.031425	.247325	.103675
36.576	163.800	1.074803	1.018777	.762635	.675496	1.953794	1.670055	.225938	.116684
36.576	168.800	1.107612	1.029135	.772824	.679605	1.896177	2.015520	.263568	.116214
36.576	173.800	1.140420	1.035070	.780789	.679513	1.834377	2.862912	.048408	.015533
36.576	178.800	1.173228	1.041200	.789388	.678943	1.784166	2.068618	.074529	.034028
36.576	183.800	1.206037	1.044552	.798328	.673619	1.790753	2.236818	.082388	.034660
36.576	188.800	1.238845	1.046741	.804554	.669597	1.855453	2.109940	.154674	.066578
36.576	193.800	1.271654	1.047204	.809001	.664946	2.115497	2.153188	.204615	.075696
36.576	198.800	1.304462	1.047605	.814437	.658915	1.931357	1.778668	.183274	.089903
36.576	203.802	1.337283	1.047747	.817221	.655686	1.981065	1.996984	.137580	.058602
36.576	208.800	1.370079	1.046607	.820321	.649969	1.890822	2.096912	.131732	.055988
36.578	213.800	1.402887	1.040657	.818917	.642138	1.846511	2.030523	.164824	.074078
36.578	218.800	1.435696	1.034651	.814598	.637912	1.758922	1.920697	.211553	.105522
36.576	223.800	1.468504	1.027135	.810708	.630682	1.750440	1.794031	.165895	.089020
36.576	228.800	1.501312	1.019631	.805671	.624932	1.698854	2.072470	.231481	.110790
36.576	233.798	1.534108	1.018607	.808317	.619826	1.950808	1.986950	.001302	.000566
36.576	238.800	1.566929	1.015677	.805992	.618043	1.981321	1.665917	.161509	.082455
36.576	243.800	1.599738	1.012336	.802422	.617206	2.034830	1.845594	.198803	.089205
36.576	248.800	1.632546	1.010770	.799066	.618990	2.119532	1.711042	.287508	.133592
36.576	253.800	1.665354	1.007881	.795033	.619473	2.017532	2.312144	.300118	.108415
36.578	258.800	1.698163	1.007830	.791745	.623588	2.053676	2.035053	.302486	.121963

Station 1 Inlet Survey 0207igvs
Vref = 76.7241 m/s
Blade spacing (s) = 152.4 mm

x(mm)	y(mm)	y/s	W/Vref	U/Vref	V/Vref	Tu	Tv	Re Stress	Corr.
-36.576	-76.200	-.500000	1.029356	.811974	.632671	2.095625	1.786403	.253722	.115134
-36.576	-71.200	-.467192	1.024838	.808630	.629612	2.115238	1.726868	.233761	.108715
-36.576	-66.200	-.434383	1.023768	.807108	.629824	2.128076	1.809573	.248726	.109722
-36.576	-61.200	-.401575	1.023059	.805455	.630786	2.292558	1.805386	.349777	.143561
-36.576	-56.200	-.368766	1.022842	.803072	.633467	2.204120	1.860417	.224534	.093019
-36.576	-51.200	-.335958	1.017755	.795760	.634501	2.537115	2.104461	.143971	.045807
-36.576	-46.200	-.303150	1.010498	.789893	.630219	1.921295	2.018353	.308156	.134994
-36.576	-41.200	-.270341	1.000027	.778608	.627554	1.917844	2.012590	.276233	.121575
-36.576	-36.200	-.237533	.994130	.770643	.628015	1.997861	1.970617	.295302	.127419
-36.576	-31.200	-.204724	.988262	.762506	.628686	1.866722	1.927873	.253934	.119867
-36.576	-26.200	-.171916	.982124	.754231	.629050	1.931714	1.816049	.327486	.158583
-36.576	-21.200	-.139108	.981118	.747777	.635155	1.844930	1.904201	.243156	.117579
-36.576	-16.200	-.106299	.980433	.743224	.639426	1.918581	1.932826	.214535	.098280
-36.576	-11.200	-.073491	.983891	.741130	.647123	1.995803	1.816350	.103784	.048635
-36.576	-6.200	-.040682	.990357	.742872	.654942	2.077970	1.730938	.273151	.129009
-36.576	-1.200	-.007874	.998413	.745280	.664370	2.163330	1.727621	.229269	.104210
-36.576	3.800	.024934	1.007953	.751021	.672262	2.405084	1.898549	.230714	.085834
-36.576	8.800	.057743	1.018177	.759129	.678533	2.094847	2.118962	.251018	.096065
-36.576	13.800	.090551	1.024399	.764945	.681361	2.276017	1.941293	.291563	.112099
-36.574	18.800	.123360	1.030843	.772433	.682630	1.881824	2.221996	.114158	.046379
-36.576	23.800	.156168	1.034659	.778577	.681423	1.893187	2.144801	.167043	.069885
-36.576	28.800	.188976	1.037329	.786549	.676308	2.270037	2.238477	1.141720	.381690
-36.576	33.800	.221785	1.038223	.792926	.670207	1.966780	2.061040	.170855	.071602
-36.576	38.800	.254593	1.038377	.797560	.664924	2.095414	1.777655	.203625	.092864
-36.576	43.800	.287402	1.036414	.800987	.657703	2.256725	1.830277	.334727	.137668
-36.576	48.800	.320210	1.036261	.804436	.653238	2.273214	1.960276	.494768	.188616
-36.576	53.800	.353018	1.037082	.809920	.647740	2.075712	2.011791	.331780	.134970
-36.576	58.800	.385827	1.035042	.810902	.643235	1.911636	1.838635	.290224	.140272
-36.576	63.800	.418635	1.031537	.809447	.639425	2.207751	1.869013	.340038	.139991
-36.576	68.800	.451444	1.026404	.807634	.633429	2.102280	1.702943	.161452	.076611
-36.576	73.800	.484252	1.022254	.804851	.630252	1.845259	1.807568	.251826	.128258
-36.576	78.800	.517060	1.015896	.802963	.622330	1.841403	1.562372	.039452	.023295
-36.576	83.800	.549869	1.010152	.799313	.617661	2.053924	1.661502	.207811	.103447
-36.576	88.800	.582677	1.005602	.795475	.615187	2.002616	1.805569	.208479	.097946
-36.576	93.800	.615486	1.000050	.789552	.613764	2.047215	1.687324	.269590	.132581
-36.576	98.800	.648294	1.002330	.790871	.615782	2.112291	1.748518	.437479	.201219
-36.576	103.800	.681102	.998577	.784632	.617664	2.574692	1.588199	.146041	.060671
-36.576	108.800	.713911	.992942	.777859	.617146	2.039545	1.709354	.207527	.101122
-36.576	113.800	.746719	.992103	.773498	.621265	2.103039	1.831812	.155514	.068577
-36.576	118.802	.779541	.985656	.764655	.621948	2.042578	1.747618	.282157	.134277
-36.576	123.800	.812336	.980539	.756472	.623865	1.781400	1.701093	.138782	.077800
-36.576	128.800	.845144	.977955	.750529	.626978	2.110684	1.692971	.099652	.047375
-36.576	133.800	.877953	.980110	.748093	.633223	2.313584	1.800242	.139622	.056947
-36.576	138.800	.910761	.980479	.746081	.636161	2.109626	1.777314	.084876	.038455
-36.576	143.800	.943570	.987045	.747151	.644998	1.959934	1.782626	.207972	.101120
-36.576	148.800	.976378	.995973	.749882	.655469	2.290964	1.833584	.311897	.126133
-36.576	153.800	1.009186	1.006135	.755701	.664246	2.048510	1.754447	.241130	.113975
-36.576	158.800	1.041995	1.014400	.759639	.672276	2.337264	1.778615	.341383	.139505
-36.576	163.800	1.074803	1.023358	.766333	.678230	2.024054	1.740942	.221989	.107019
-36.576	168.800	1.107612	1.033623	.775969	.682825	2.007641	1.700814	.203873	.101427
-36.576	173.800	1.140420	1.039972	.784553	.682656	1.809061	1.973621	.141581	.067363
-36.576	178.800	1.173228	1.045980	.794719	.680071	1.918253	2.025202	.154453	.067539
-36.578	183.800	1.206037	1.051276	.805435	.675614	1.831189	1.712189	.162420	.088002
-36.578	188.800	1.238845	1.051958	.810524	.670573	1.825907	1.718584	.214557	.116153
-36.578	193.800	1.271654	1.052761	.815284	.666046	2.327724	2.035491	.057701	.020688
-36.576	198.800	1.304462	1.052928	.820217	.660228	2.218178	1.926063	.236078	.093870
-36.576	203.800	1.337270	1.053267	.824341	.655617	2.377877	1.760823	.263543	.106926
-36.578	208.800	1.370079	1.050363	.824783	.650381	1.984105	2.087684	.159916	.065584
-36.574	213.800	1.402887	1.044522	.822804	.643443	1.822182	1.988433	.361619	.169545
-36.576	218.800	1.435696	1.036709	.818748	.635938	1.863921	1.796424	.234312	.118876
-36.576	223.800	1.468504	1.028846	.814250	.628904	1.839033	1.779088	.173114	.089884
-36.576	228.800	1.501312	1.025655	.811529	.627208	1.958503	1.681985	.186889	.096377
-36.576	233.800	1.534121	1.019283	.807306	.622250	2.071046	1.542745	.062206	.033074
-36.578	238.800	1.566929	1.017584	.806555	.620440	2.294996	1.663778	.196239	.087306
-36.578	243.800	1.599738	1.015137	.804012	.619732	2.056116	1.726729	.310711	.148670
-36.578	248.800	1.632546	1.018606	.806002	.622830	2.383107	1.688182	.386105	.163034
-36.576	253.800	1.665354	1.013986	.799699	.623417	2.859516	1.688344	.278009	.097823
-36.574	258.800	1.698163	1.012355	.794677	.627177	2.367582	1.789587	.266689	.106926

Station 3 Inlet survey 0301inl3
Vref = 76.6737 m/s
Blade spacing (s) = 152.4 mm

x(mm)	y(mm)	y/s	W/Vref	U/Vref	V/Vref	Tu	Tv	Re Stres	Cuv
-6.102	-76.200	-.500000	1.039541	.848074	.601177	1.886567	1.979629	.359664	.163813
-6.102	-71.200	-.467192	1.023684	.835391	.591651	1.893012	1.960810	.417797	.191462
-6.102	-66.200	-.434383	1.008597	.822416	.583865	1.823165	1.815569	.138653	.071252
-6.102	-61.200	-.401575	.996574	.811977	.577799	1.858462	1.730601	.022497	.011898
-6.102	-56.200	-.368766	.980548	.797294	.570785	1.868324	1.745957	.186900	.097461
-6.100	-51.200	-.335958	.970586	.786800	.568315	2.201121	1.761145	.265435	.116473
-6.100	-46.200	-.303150	.962805	.776750	.568904	2.222088	1.749916	.245668	.107467
-6.102	-41.200	-.270341	.952507	.763092	.570052	2.260844	1.716210	.249799	.109510
-6.100	-36.200	-.237533	.946976	.753656	.573382	2.198822	1.869288	.407790	.168763
-6.100	-31.200	-.204724	.936675	.737381	.577607	2.147599	1.803192	.311978	.137036
-6.100	-26.200	-.171916	.924027	.718848	.580589	1.992099	1.775261	.227059	.109213
-6.100	-21.200	-.139108	.911271	.697216	.586775	1.971189	2.016076	.291829	.124911
-6.100	-16.200	-.106299	.894140	.667175	.595284	1.887266	1.883001	.198382	.094957
-6.100	-11.200	-.073491	.882373	.636835	.610756	1.881090	1.950796	.236725	.109731
-6.100	-6.200	-.040682	.884068	.600368	.648949	1.967699	1.916715	.202878	.091501
-6.100	-1.200	-.007874	.934210	.581480	.731184	1.972391	2.455287	.034880	.012251
-6.100	3.800	.024934	1.034496	.643103	.810309	1.763743	2.805193	-.189880	-.065281
-6.100	8.800	.057743	1.098038	.725099	.824572	2.038434	2.877608	.047554	.013790
-6.100	13.800	.090551	1.122898	.781359	.806460	1.961282	2.430454	.297196	.106053
-6.100	18.800	.123360	1.132740	.819970	.781505	2.012213	1.688434	.264977	.132665
-6.100	23.800	.156168	1.130677	.841986	.754646	1.952027	2.170860	.106548	.042770
-6.100	28.800	.188976	1.125252	.855844	.730565	2.075566	2.234834	.093772	.034387
-6.100	33.800	.221785	1.117148	.864962	.707009	1.925240	1.703093	.097089	.050368
-6.100	38.800	.254593	1.105875	.866156	.687556	2.107159	1.799521	.151212	.067833
-6.100	43.800	.287402	1.092045	.866297	.664899	2.048654	2.159633	.092383	.035518
-6.100	48.800	.320210	1.078050	.863973	.644780	1.961849	1.832279	.155825	.073737
-6.100	53.800	.353018	1.062016	.857967	.625916	1.815664	1.711956	.211677	.115839
-6.100	58.800	.385827	1.049383	.852946	.611301	1.851933	1.579412	.200223	.116439
-6.100	63.800	.418635	1.036904	.844419	.601770	2.623136	1.623857	.209725	.083751
-6.100	68.800	.451444	1.027054	.839134	.592195	2.019552	1.702301	.238123	.117819
-6.100	73.800	.484252	1.023724	.839370	.586063	1.845926	1.696171	.215274	.116954
-6.100	78.800	.517060	1.010392	.828375	.578520	2.088690	1.699872	.161224	.077241
-6.100	83.800	.549869	.996143	.816599	.570497	2.057716	1.674340	.114545	.056553
-6.102	88.800	.582677	.983978	.805022	.565820	1.778446	1.615433	.159870	.094655
-6.102	93.800	.615486	.972797	.794109	.561893	2.033674	1.653606	.061864	.031292
-6.102	98.800	.648294	.963174	.785231	.557777	1.792259	1.630030	.149684	.087154
-6.102	103.800	.681102	.950626	.774029	.551876	1.879227	1.612638	.227202	.127527
-6.100	108.800	.713911	.939812	.760300	.552441	1.925657	1.597698	.189969	.105031
-6.100	113.800	.746719	.932267	.749691	.554152	2.080348	1.730933	.325359	.153692
-6.100	118.800	.779528	.922974	.734959	.558315	2.184356	1.688290	.277755	.128115
-6.100	123.800	.812336	.914790	.720068	.564218	2.211956	1.837930	.324575	.135805
-6.100	128.800	.845144	.904157	.699695	.572649	2.037848	1.597558	.254272	.132855
-6.100	133.800	.877953	.892718	.676885	.582041	2.001245	1.679880	.261366	.132245
-6.100	138.800	.910761	.881622	.650102	.595504	1.913776	1.660283	.232089	.124248
-6.102	143.800	.943570	.874764	.620599	.616498	1.818416	1.598124	.136665	.079995
-6.102	148.800	.976378	.891927	.587264	.671308	1.935857	1.743663	.145978	.073563
-6.102	153.800	1.009186	.974222	.603302	.764942	1.899135	2.595737	-.306117	-.105628
-6.102	158.800	1.041995	1.059583	.680798	.811930	1.857203	1.990423	.072139	.033195
-6.100	163.800	1.074803	1.106368	.750990	.812443	2.007840	2.277684	.167593	.062336
-6.100	168.800	1.107612	1.126404	.801884	.791055	1.851397	1.752898	.100322	.052583
-6.100	173.800	1.140420	1.129587	.831026	.765090	2.105918	2.158190	.096340	.036056
-6.100	178.800	1.173228	1.130297	.851576	.743229	2.196964	1.715483	.170998	.077177
-6.102	183.800	1.206037	1.122612	.862979	.718000	1.945025	1.594333	.155112	.085084
-6.102	188.800	1.238845	1.117621	.871747	.699381	1.893104	1.650853	.183986	.100141
-6.100	193.800	1.271654	1.105759	.873396	.678146	2.112212	2.044476	.175523	.069139
-6.100	198.800	1.304462	1.093967	.872340	.660142	2.128081	1.718705	.192296	.089431
-6.100	203.800	1.337270	1.080889	.870490	.640756	1.860734	2.193242	.194479	.081060
-6.100	208.800	1.370079	1.068376	.865976	.625710	1.806703	2.286907	.221122	.091034
-6.102	213.800	1.402887	1.057796	.860963	.614554	1.928324	1.632777	.137842	.074470
-6.102	218.800	1.435696	1.047524	.855237	.604878	2.039210	1.560433	.175701	.093923

Station 6 Boundary Layer Survey 0211bl63
Vref = 76.0511 m/s
Blade Chord (c) = 127.254 mm

x(mm)	y(mm)	d/c	W/Vref	U/Vref	V/Vref	Tu	Tv	Re Stress	Corr.
29.450	30.588	.003930	1.307904	1.121743	.672536	2.736717	2.276474	.045605	.012657
29.194	31.016	.007859	1.323205	1.133531	.682625	1.506202	1.552727	.219317	.162137
28.938	31.446	.011788	1.322661	1.134264	.680350	1.650649	2.473319	.394840	.167215
28.680	31.876	.015717	1.318951	1.130369	.679631	1.606853	1.762984	.241686	.147508
28.424	32.304	.019646	1.314357	1.126598	.676987	1.624881	1.754222	.143693	.087161
28.166	32.732	.023576	1.307881	1.122006	.672052	2.072581	2.265521	.164487	.060568
27.910	33.162	.027505	1.303050	1.118372	.668719	1.879636	2.165392	.129909	.055185
27.652	33.590	.031434	1.297769	1.114752	.664480	1.807904	1.999087	.027397	.013107
27.396	34.020	.035363	1.292790	1.111113	.660858	1.930226	1.864665	.029827	.014328
27.140	34.448	.039292	1.289344	1.108522	.658474	1.717178	2.272171	.082667	.036633
26.882	34.878	.043221	1.287229	1.104931	.660368	1.737835	1.923566	.122286	.063248
26.624	35.306	.047151	1.280069	1.099988	.654678	1.761510	1.883470	.104368	.054389
26.368	35.736	.051080	1.277107	1.097783	.652591	1.808257	2.023621	-.112801	-.053298
26.110	36.164	.055009	1.272563	1.093683	.650595	1.893614	2.265764	-.014982	-.006038
25.854	36.594	.058938	1.267547	1.089149	.648406	1.907166	2.050072	.234958	.103902
25.596	37.024	.062867	1.263673	1.085777	.646497	1.909599	1.990060	.223021	.101468
25.338	37.452	.066796	1.256772	1.079834	.642987	1.821389	2.067944	-.021552	-.009893
25.082	37.880	.070725	1.252966	1.076592	.640994	1.761078	1.925399	.108506	.055328
24.826	38.310	.074655	1.249159	1.072627	.640209	2.390672	2.016658	-.013996	-.005019
24.570	38.740	.078584	1.245777	1.070041	.637945	2.110046	2.104605	.014862	.005786
24.310	39.168	.082513	1.241254	1.066346	.635308	1.936037	2.065171	.134882	.058327
24.056	39.596	.086442	1.237826	1.063004	.634221	1.850211	1.975326	.125466	.059354
23.798	40.026	.090371	1.234303	1.060924	.630830	2.165971	1.798073	.039743	.017644
23.540	40.454	.094300	1.229635	1.055889	.630159	1.780418	1.851401	.105747	.055467
23.284	40.884	.098229	1.226101	1.052203	.629437	1.920534	1.834923	.145918	.071591
23.028	41.312	.102159	1.222617	1.049434	.627281	1.870500	1.805277	.019197	.009829
22.770	41.742	.106088	1.216958	1.043356	.626414	2.620442	1.746011	.146879	.055504
22.512	42.170	.110017	1.215185	1.042492	.624408	2.007955	1.743727	.074973	.037022
22.256	42.600	.113946	1.211753	1.039730	.622341	1.988962	1.791408	.000954	.000463
21.998	43.028	.117875	1.206918	1.034640	.621427	2.015085	1.939629	.082329	.036419
21.742	43.458	.121804	1.204966	1.033262	.619929	1.885135	1.833651	.185727	.092898
21.486	43.886	.125733	1.200544	1.028703	.618931	2.052561	1.707619	.235048	.115947
21.226	44.316	.129663	1.198178	1.025553	.619574	1.922203	1.676134	.194304	.104270
20.972	44.744	.133592	1.196686	1.024234	.618872	2.311982	1.715476	.265056	.115547
20.714	45.174	.137521	1.192318	1.020476	.616646	1.906177	1.678683	.096945	.052382
20.458	45.602	.141450	1.188925	1.016457	.616731	2.163418	1.733768	.193759	.089314
20.200	46.032	.145379	1.185480	1.013902	.614300	2.065370	1.814894	.148660	.068570
19.944	46.460	.149308	1.181835	1.011185	.611752	1.924234	1.672058	.078747	.042317

Station 7 Boundary Layer Survey 0211bl73
Vref = 76.2682 m/s
Blade Chorde (c) = 127.254 mm

x(mm)	y(mm)	d/c	W/Vref	U/Vref	V/Vref	Tu	Tv	Re Stress	Corr.
60.4700	41.9420	.003957	.419257	.409767	.088700	17.82829	5.03187	1.66156	.03202
60.3180	42.4220	.007913	.665341	.648118	.150403	14.95785	5.06287	4.50350	.10282
60.1660	42.9020	.011870	.926820	.897508	.231243	13.37907	4.02409	.78528	.02522
60.0140	43.3820	.015827	1.068254	1.031080	.279354	5.69097	2.64177	-.92383	-.10624
59.8640	43.8620	.019783	1.095062	1.054052	.296877	3.22088	2.02954	-1.33127	-.35211
59.7100	44.3420	.023740	1.096796	1.054219	.302628	2.89159	1.83769	-1.26241	-.41075
59.5580	44.8220	.027697	1.098242	1.054207	.307868	2.91298	1.82786	-1.22532	-.39789
59.4060	45.3020	.031653	1.099797	1.054703	.311698	2.76318	1.75408	-1.13879	-.40624
59.2540	45.7820	.035610	1.100892	1.054165	.317331	2.67323	1.74980	-.85425	-.31576
59.1020	46.2620	.039566	1.099794	1.051109	.323600	2.58013	1.84764	-.88686	-.32165
58.9500	46.7420	.043523	1.103165	1.053720	.326569	2.55663	1.79260	-.79432	-.29966
58.7980	47.2220	.047480	1.102732	1.052558	.328846	2.48452	1.81177	-.73494	-.28229
58.6460	47.7020	.051436	1.102355	1.050918	.332803	2.51601	1.80864	-.58525	-.22236
58.4940	48.1820	.055393	1.101395	1.049187	.335079	2.43965	1.82451	-.57970	-.22517
58.3420	48.6620	.059350	1.103546	1.049592	.340838	2.42659	1.82098	-.38327	-.14997
58.1900	49.1420	.063306	1.101235	1.046399	.343172	2.68589	1.85832	-.68614	-.23768
58.0400	49.6220	.067263	1.102045	1.046310	.346033	2.28031	1.79422	-.36805	-.15554
57.8860	50.1020	.071220	1.100780	1.044938	.346151	2.22403	1.84108	-.38633	-.16313
57.7340	50.5820	.075176	1.099425	1.042783	.348337	2.52581	1.75957	-.31441	-.12231
57.5800	51.0620	.079133	1.099576	1.042001	.351144	2.26603	1.83908	-.43625	-.18099
57.4280	51.5420	.083090	1.101698	1.042954	.354944	2.20178	1.86186	-.29880	-.12602
57.2780	52.0220	.087046	1.100607	1.040894	.357599	2.56460	1.78374	-.37223	-.14069
57.1240	52.5020	.091003	1.098926	1.038595	.359107	2.15361	1.79556	-.33079	-.14790
56.9740	52.9820	.094960	1.099179	1.037303	.363590	2.26626	1.93881	-.41103	-.16174
56.8240	53.4620	.098916	1.097236	1.035112	.363966	2.25036	1.99396	-.39686	-.15292
56.6680	53.9420	.102873	1.094456	1.031718	.365228	2.52652	1.93000	-.15962	-.05660
56.5180	54.4220	.106830	1.093754	1.030616	.366235	2.16929	1.84610	-.16356	-.07061
56.3660	54.9020	.110786	1.094550	1.030696	.368380	2.16666	1.84322	-.22930	-.09927
56.2120	55.3820	.114743	1.093016	1.028474	.370034	2.20761	1.76899	-.19246	-.08521
56.0620	55.8620	.118700	1.089932	1.024739	.371299	2.49237	1.70145	-.08934	-.03642
55.9080	56.3420	.122656	1.088842	1.022995	.372906	2.24611	1.75303	-.27813	-.12213
55.7560	56.8220	.126613	1.086982	1.020669	.373851	2.23927	1.89380	-.08747	-.03566
55.6060	57.3020	.130570	1.085918	1.018887	.375616	2.31991	1.78709	-.05598	-.02335
55.4540	57.7820	.134526	1.085796	1.017649	.378609	2.43075	1.75075	-.09398	-.03818
55.3020	58.2620	.138483	1.083572	1.014772	.379958	2.14646	1.80080	.06430	.02876
55.1520	58.7420	.142439	1.081508	1.012212	.380904	2.52160	1.84057	.06427	.02394
54.9980	59.2220	.146396	1.082751	1.012780	.382920	2.13614	1.77926	-.17224	-.07835
54.8460	59.7020	.150353	1.080372	1.010006	.383525	2.41662	1.90417	-.11595	-.04356
54.6940	60.1820	.154309	1.077736	1.006710	.384773	2.60450	1.72686	.18734	.07202
54.5420	60.6620	.158266	1.076731	1.005342	.385534	2.13460	1.85170	-.13295	-.05816

Station 8 Blade #3 Boundary Layer Survey **0204bl83**
Vref = **76.677 m/s**
Blade Chord (c) = **127.254 mm**

x(mm)	y(mm)	d/c	W/Vref	U/Vref	V/Vref	Tu	Tv	Re Stress	Corr.
91.538	42.252	.003930	.127887	-.126629	.017891	5.81246	3.27314	-.22790	-.02037
91.572	42.752	.007851	.130135	-.126363	.031105	5.22337	5.46861	-.34718	-.02067
91.606	43.250	.011772	.136139	-.134683	.019855	5.01582	4.28431	-1.50041	-.11876
91.638	43.750	.015694	.134131	-.132574	.020374	4.81702	4.83582	-1.04260	-.07613
91.670	44.248	.019615	.131503	-.128164	.029445	5.08727	5.01818	-.38117	-.02540
91.704	44.748	.023536	.131433	-.129991	.019417	5.21895	5.12457	-1.59613	-.10151
91.736	45.248	.027458	.125682	-.122315	.028894	5.33131	5.52682	-1.55455	-.08974
91.770	45.746	.031379	.129031	-.126776	.024016	5.20461	5.62996	-2.51542	-.14601
91.802	46.244	.035300	.124935	-.121074	.030817	5.79992	5.64627	-.77477	-.04024
91.836	46.744	.039221	.116563	-.111537	.033860	5.90192	5.84036	-.90722	-.04477
91.870	47.244	.043143	.110813	-.105188	.034859	6.39151	6.11196	-.58114	-.02530
91.900	47.742	.047064	.107228	-.096051	.047665	7.70147	7.10186	1.26543	.03935
91.934	48.240	.050985	.096777	-.078400	.056739	8.76107	7.44651	.17312	.00451
91.968	48.740	.054907	.080519	-.053780	.059925	10.48632	8.35900	.68393	.01327
92.000	49.238	.058828	.063907	-.029946	.056457	11.58217	8.12114	.03038	.00055
92.034	49.738	.062749	.066012	.004266	.065874	14.53307	8.35564	-.64897	-.00909
92.068	50.238	.066671	.110298	.045948	.100272	16.46236	8.89957	4.34900	.05049
92.100	50.736	.070592	.154031	.107059	.110743	19.55691	9.23325	.02824	.00027
92.132	51.234	.074513	.188379	.154886	.107224	22.71776	8.91520	-2.71706	-.02282
92.166	51.734	.078434	.278043	.245320	.130866	25.27262	9.43571	2.01935	.01440
92.198	52.234	.082356	.329181	.295039	.145986	27.06743	9.96127	12.71570	.08021
92.232	52.732	.086277	.417861	.388036	.155037	28.47222	9.75698	4.14455	.02538
92.266	53.230	.090198	.540280	.510484	.176941	29.44468	9.94649	8.05979	.04681
92.298	53.730	.094120	.612400	.580744	.194345	27.81078	10.04401	16.50810	.10052
92.332	54.230	.098041	.697969	.663925	.215321	27.25639	10.27473	27.71510	.16833
92.364	54.728	.101962	.769968	.731776	.239486	25.98288	9.84852	19.18870	.12754
92.396	55.228	.105883	.854181	.813676	.259919	23.91946	9.21262	15.13550	.11682
92.430	55.726	.109805	.905928	.861473	.280300	20.45026	8.90515	12.91540	.12063
92.464	56.224	.113726	.937711	.890429	.294006	18.49563	8.59012	10.79240	.11554
92.496	56.724	.117647	.969544	.921433	.301625	15.84910	7.84343	9.97491	.13648
92.528	57.224	.121569	.993200	.942558	.313099	13.60252	6.96627	4.92223	.08835
92.562	57.722	.125490	1.007312	.955777	.318071	10.91115	6.34710	-.76067	-.01868
92.594	58.220	.129411	1.014401	.961672	.322796	9.32084	6.32980	-2.70886	-.07809
92.628	58.720	.133332	1.022613	.970882	.321131	7.18032	5.72471	-3.01399	-.12471
92.660	59.220	.137254	1.023177	.971161	.322085	6.26695	5.75086	-2.44513	-.11539
92.694	59.718	.141175	1.024338	.972944	.320388	6.25156	5.08764	-1.40707	-.07525
92.726	60.218	.145096	1.024023	.973124	.318832	5.13101	4.82269	-2.10099	-.14441
92.760	60.716	.149018	1.026081	.975909	.316927	4.25611	4.22914	-1.04984	-.09920
92.792	61.214	.152939	1.023842	.973707	.316461	4.11168	4.29511	-1.35340	-.13035
92.826	61.714	.156860	1.021233	.971244	.315598	3.81732	3.98313	-1.02520	-.11468
92.858	62.214	.160782	1.022324	.972349	.315727	3.65068	3.77922	-1.16012	-.14302
92.892	62.712	.164703	1.021580	.972088	.314118	3.23447	3.73323	-.73737	-.10386
92.924	63.210	.168624	1.019366	.971217	.309587	3.21140	3.41295	-.72044	-.11180

Station 8 Blade #4 Boundary Layer Survey 0207bl84
Vref = 76.8688 m/s
Blade Chord (c) = 127.254 mm

x(mm)	y(mm)	d/c	W/Vref	U/Vref	V/Vref	Tu	Tv	Re Stress	Corr.
91.536	91.536	.00392	.12305	-.12139	.02009	6.27298	3.52075	-.64944	-.04977
91.570	91.570	.01040	.12828	-.12653	.02106	5.98525	4.23124	-1.15726	-.07734
91.602	91.602	.01688	.12947	-.12802	.01933	6.38274	5.22924	-1.17361	-.05951
91.636	91.636	.02336	.13383	-.13244	.01925	6.25959	5.64923	-.78247	-.03745
91.670	91.670	.02984	.12979	-.12798	.02160	5.80768	5.74422	-.88577	-.04494
91.702	91.702	.03632	.12455	-.12347	.01638	6.55868	6.28313	-1.01399	-.04164
91.734	91.734	.04279	.12636	-.12533	.01611	6.36832	6.02156	-1.35710	-.05989
91.768	91.768	.04927	.12184	-.12033	.01913	7.32612	6.64872	-2.83879	-.09863
91.802	91.802	.05575	.11355	-.11185	.01954	7.91272	7.46767	-2.26189	-.06478
91.834	91.834	.06223	.09522	-.09157	.02612	10.30969	7.55441	-2.47136	-.05370
91.868	91.868	.06871	.07471	-.07161	.02130	11.56570	7.55385	-2.18890	-.04240
91.900	91.900	.07519	.06370	-.05757	.02726	12.25185	8.40250	-2.54800	-.04189
91.934	91.934	.08167	.05002	-.04068	.02910	12.36565	8.88441	-2.79108	-.04300
91.966	91.966	.08814	.04490	-.01968	.04036	14.87180	9.36076	-3.75542	-.04565
92.000	92.000	.09462	.05402	.02021	.05009	16.94820	9.96361	1.32853	.01331
92.034	92.034	.10110	.08003	.06061	.05227	18.92412	10.24789	-.85471	-.00746
92.064	92.064	.10758	.11900	.10090	.06309	20.56241	10.06446	.40685	.00333
92.096	92.096	.11406	.19918	.18303	.07856	24.30270	10.76549	-7.33428	-.04744
92.132	92.132	.12054	.26757	.25152	.09126	25.91860	10.95924	8.45644	.05038
92.164	92.164	.12702	.32581	.30794	.10642	27.20615	10.92776	6.32552	.03601
92.196	92.196	.13349	.41689	.39843	.12265	29.17626	11.41943	26.51230	.13467
92.230	92.230	.13997	.51356	.49261	.14519	29.22227	11.32751	35.55840	.18180
92.264	92.264	.14645	.56861	.54429	.16449	29.32761	11.45006	34.91880	.17599
92.296	92.296	.15293	.64255	.61396	.18954	29.12800	11.42980	26.60770	.13526
92.330	92.330	.15941	.71081	.67936	.20909	27.04251	10.77896	39.44420	.22901
92.362	92.362	.16589	.81141	.77399	.24357	25.44579	10.52080	30.24360	.19119
92.396	92.396	.17237	.85414	.81093	.26823	23.35389	9.57868	19.75860	.14948
92.428	92.428	.17884	.89077	.84516	.28140	22.46343	9.83989	12.91440	.09888
92.460	92.460	.18532	.94188	.89321	.29886	17.97229	8.81078	8.85479	.09464
92.494	92.494	.19180	.96509	.91677	.30154	16.04462	7.97709	6.65738	.08803
92.528	92.528	.19828	.98221	.93020	.31537	14.32866	7.54541	4.38371	.06862
92.558	92.558	.20476	.99843	.94577	.31999	11.14692	6.96311	-2.69649	-.05880
92.594	92.594	.21124	1.00846	.95466	.32498	9.77574	6.43049	-4.03098	-.10852
92.626	92.626	.21772	1.00952	.95618	.32380	9.42337	6.34045	-3.21497	-.09106
92.660	92.660	.22419	1.01582	.96235	.32522	7.18191	5.93365	-3.72638	-.14799
92.692	92.692	.23067	1.01804	.96683	.31881	6.17744	5.66336	-2.13306	-.10319
92.726	92.726	.23715	1.01930	.96716	.32182	5.57158	5.29602	-4.48120	-.25702
92.758	92.758	.24363	1.02075	.97085	.31525	5.27861	4.89266	-2.52311	-.16534
92.790	92.790	.25011	1.01827	.96762	.31715	4.58447	4.72497	-1.51769	-.11858
92.824	92.824	.25659	1.01486	.96600	.31112	4.10838	4.44234	-1.51469	-.14046
92.858	92.858	.26307	1.01665	.96793	.31094	3.74795	3.96416	-.60652	-.06909
92.890	92.890	.26954	1.01465	.96715	.30682	4.06993	4.22635	-1.53799	-.15132
92.924	92.924	.27602	1.01526	.96745	.30788	3.42792	3.75158	-1.14853	-.15115

Station 9 Boundary Layer Survey 0218bl93
Vref = 76.3697 m/s
Blade Chord (c) = 127.254 mm

x(mm)	y(mm)	d/c	W/Vref	U/Vref	V/Vref	Tu	Tv	Re Stress	Corr.
115.980	40.214	.00396	.19963	-.17139	.10236	6.05498	4.63249	-10.5086	-.64236
116.020	40.716	.00791	.17335	-.14169	.09986	5.12421	6.40990	-1.01691	-.05308
116.062	41.218	.01187	.16438	-.13742	.09020	5.45814	6.68885	.15867	.00745
116.100	41.720	.01583	.16132	-.13482	.08860	5.33037	7.82360	-.59046	-.02428
116.142	42.222	.01979	.15554	-.12815	.08815	5.86572	8.26324	-.21564	-.00763
116.180	42.724	.02374	.14994	-.12562	.08188	5.72687	8.44725	.12843	.00455
116.222	43.226	.02770	.14889	-.12309	.08377	5.83429	8.69263	.35839	.01212
116.260	43.728	.03166	.14527	-.12040	.08130	6.06648	9.11677	.55783	.01729
116.300	44.230	.03562	.13962	-.11330	.08159	6.51135	9.16124	.32836	.00944
116.340	44.732	.03957	.13905	-.11365	.08013	6.49012	9.83053	-.18281	-.00491
116.380	45.234	.04353	.13399	-.10849	.07864	6.50226	10.00300	-1.06230	-.02800
116.420	45.736	.04749	.13507	-.10745	.08185	6.90738	10.14798	2.79404	.06834
116.460	46.240	.05145	.12877	-.10113	.07972	6.65363	10.19569	-1.26501	-.03197
116.500	46.742	.05540	.12305	-.09411	.07928	7.42007	10.68371	3.77819	.08172
116.540	47.242	.05936	.12233	-.09242	.08014	8.20997	11.33866	3.79911	.06997
116.580	47.744	.06332	.11544	-.08850	.07413	8.05714	11.20423	4.99176	.09481
116.618	48.246	.06728	.11985	-.08864	.08066	8.00302	12.14429	7.56524	.13346
116.660	48.748	.07123	.11500	-.07755	.08492	8.76806	12.59166	9.94855	.15450
116.698	49.250	.07519	.10830	-.06481	.08676	10.29996	13.25122	9.57927	.12034
116.740	49.752	.07915	.09519	-.05839	.07517	10.18863	13.02669	13.22310	.17082
116.780	50.254	.08310	.09110	-.05194	.07485	11.27491	13.70757	15.79140	.17519
116.820	50.756	.08706	.09536	-.04364	.08478	11.60896	14.59641	24.93050	.25226
116.862	51.258	.09102	.09885	-.03205	.09351	12.26657	15.85776	26.79230	.23616
116.900	51.762	.09498	.11151	-.01237	.11083	12.83544	17.13178	34.24760	.26704
116.942	52.262	.09893	.10276	.01331	.10190	14.85635	17.06390	44.12630	.29845
116.980	52.764	.10289	.10252	.01693	.10111	14.70064	17.14519	43.86440	.29840
117.020	53.266	.10685	.11636	.04576	.10699	16.76982	18.00998	43.17800	.24512
117.060	53.768	.11081	.14068	.07951	.11605	18.17333	17.91362	48.98400	.25799
117.098	54.270	.11476	.14353	.08706	.11411	19.12039	18.01924	61.74270	.30726
117.140	54.772	.11872	.17573	.13460	.11298	21.22353	18.91981	71.68230	.30608
117.180	55.274	.12268	.19689	.15566	.12057	21.77425	18.76892	66.11810	.27739
117.218	55.776	.12664	.22320	.18548	.12417	22.36600	18.74273	73.95410	.30248
117.260	56.278	.13059	.24654	.21387	.12266	23.17105	18.32755	74.72750	.30171
117.300	56.780	.13455	.28875	.26109	.12332	24.17959	18.05899	67.75460	.26604
117.340	57.282	.13851	.32245	.29737	.12468	26.01237	17.95421	89.92000	.33012
117.378	57.786	.14247	.35434	.32916	.13119	25.96688	17.71862	68.55490	.25547
117.420	58.286	.14642	.38692	.36872	.11727	26.98233	16.30959	59.35160	.23124
117.462	58.788	.15038	.45267	.43829	.11318	27.02541	15.57400	57.49990	.23424
117.500	59.290	.15434	.46894	.45404	.11729	28.59623	15.20094	40.22280	.15865
117.542	59.792	.15829	.51594	.50504	.10548	27.32392	14.87037	23.62770	.09970
117.580	60.294	.16225	.53873	.53061	.09317	27.77188	13.60281	27.38850	.12431
117.620	60.796	.16621	.60683	.59991	.09141	26.87438	12.94454	21.45790	.10576
117.662	61.298	.17017	.62290	.61739	.08264	28.03655	12.36764	23.33300	.11538
117.700	61.800	.17412	.64265	.63803	.07692	27.17129	12.14408	-.56607	-.00294
117.740	62.302	.17808	.69720	.69424	.06419	25.34448	11.40596	16.47940	.09774
117.780	62.804	.18204	.71394	.71048	.07022	26.82398	11.18290	-5.67174	-.03242
117.820	63.306	.18600	.76837	.76643	.05448	25.00661	9.77083	-4.74060	-.03327
117.860	63.808	.18995	.78861	.78717	.04759	24.50998	9.26204	-2.16667	-.01636
117.902	64.310	.19391	.82513	.82415	.04032	22.60254	9.08752	3.50509	.02926
117.940	64.812	.19787	.84445	.84393	.02956	21.20557	8.21398	5.33605	.05253
117.978	65.314	.20183	.84361	.84303	.03128	22.16500	7.92289	-3.49396	-.03411
118.020	65.816	.20578	.88421	.88400	.01958	19.99425	7.27039	-5.32733	-.06284
118.060	66.318	.20974	.90161	.90150	.01413	18.50454	6.78531	-.02791	-.00038
118.100	66.820	.21370	.91838	.91832	.01032	17.88015	6.86598	-1.09901	-.01535
118.140	67.322	.21766	.93739	.93739	-.00022	15.18399	6.20505	-5.38976	-.09808
118.180	67.824	.22161	.94032	.94032	-.00103	14.55671	6.19617	-5.62182	-.10687
118.220	68.326	.22557	.94834	.94827	-.01160	14.39041	5.54221	-4.73872	-.10187
118.260	68.828	.22953	.95977	.95965	-.01559	13.62995	5.55325	-6.21566	-.14080

Station 11 Wake Survey **0302WK11**
Vref = **77.4166 m/s**
Blade spacing (s) = **152.4 mm**

x(mm)	y(mm)	y/s	W/Vref	U/Vref	V/Vref	Tu	Tv	Re stress	Corr.
128.13	-14.22	-.09331	.88115	.86676	.15858	1.84745	1.88715	.46659	.22330
128.13	-9.22	-.06050	.87699	.86407	.14997	1.75382	1.80279	.40768	.21514
128.13	-4.22	-.02769	.87355	.86206	.14121	1.73989	1.75356	.34797	.19030
128.13	0.78	.00512	.87656	.86645	.13271	1.82474	2.15256	.22295	.09471
128.13	5.78	.03793	.88149	.87310	.12136	1.84264	1.92069	.32403	.15277
128.13	10.78	.07073	.89198	.88526	.10928	1.87720	2.05773	.49335	.21310
128.13	15.78	.10354	.90984	.90462	.09730	1.92623	2.16339	.45223	.18107
128.13	20.78	.13635	.93035	.92673	.08208	1.99256	2.55550	.40442	.13252
128.13	25.78	.16916	.96526	.96299	.06612	1.92309	2.46829	.46181	.16233
128.13	30.78	.20197	1.01283	1.01141	.05369	2.45440	2.82555	.85735	.20627
128.13	35.78	.23478	.00697	-.00309	-.00624	11.6780	10.2004	25.29580	.35432
128.13	40.78	.26759	.08566	-.08516	.00927	8.38972	9.80439	3.28917	.06672
128.13	45.78	.30039	.07044	-.06367	.03014	10.8646	11.21788	-3.18165	-.04356
128.13	50.78	.33320	.05289	.02932	.04402	16.64494	13.30795	-13.6492	-.10281
128.13	55.78	.36601	.30248	.28910	.08896	26.25414	15.74312	-52.4008	-.21153
128.13	60.78	.39882	.66779	.65811	.11326	25.58403	14.85269	-46.7554	-.20530
128.13	65.78	.43163	.91291	.90246	.13775	16.58974	11.09954	-24.9835	-.22638
128.13	70.78	.46444	.96905	.95703	.15211	7.54147	6.93333	-4.26932	-.13624
128.13	75.78	.49724	.96263	.94882	.16248	3.96533	4.01966	-.47412	-.04963
128.13	80.78	.53005	.94699	.93248	.16515	2.60960	2.69392	.09948	.02361
128.13	85.78	.56286	.93350	.91817	.16849	2.13187	2.43639	.29615	.09513
128.13	90.78	.59567	.91945	.90387	.16854	1.95885	2.01832	.42690	.18016
128.13	95.78	.62848	.90975	.89390	.16911	1.86001	2.11325	.40674	.17266
128.13	100.78	.66129	.89573	.88001	.16704	1.80898	1.93156	.45288	.21626
128.13	105.78	.69409	.88653	.87110	.16466	2.04684	1.81830	.28609	.12826
128.13	110.78	.72689	.87798	.86245	.16443	1.73718	1.87488	.38018	.19476
128.13	115.78	.75971	.87274	.85792	.16013	1.86709	1.62302	.31430	.17306
128.13	120.78	.79252	.86700	.85251	.15782	1.81228	1.71648	.33196	.17806
128.13	125.78	.82533	.86493	.85067	.15643	1.90913	1.64360	.48230	.25646
128.13	130.78	.85814	.86223	.84841	.15371	1.75476	1.58323	.27567	.16556
128.13	135.78	.89094	.86048	.84743	.14929	1.81857	1.60279	.19780	.11323
128.13	140.78	.92375	.85914	.84729	.14221	1.69261	1.65530	.32303	.19237
128.13	145.78	.95656	.85770	.84667	.13706	1.69708	1.69297	.30664	.17808
128.13	150.78	.98937	.85904	.84968	.12649	1.61314	1.70060	.21745	.13226
128.13	155.78	1.02218	.86205	.85435	.11496	1.66453	1.79851	.30800	.17166
128.13	160.78	1.05499	.87128	.86539	.10113	1.69995	1.90905	.50162	.25790
128.13	165.78	1.08780	.88473	.88025	.08887	1.70574	1.96783	.37413	.18597
128.13	170.78	1.12060	.90239	.89941	.07329	1.78744	2.10285	.44353	.19689
128.13	175.78	1.15341	.92849	.92679	.05615	1.92662	2.61061	.62915	.20871
128.13	180.78	1.18622	.96773	.96698	.03808	2.14382	2.95117	.66043	.17417
128.13	185.78	1.21903	.85369	.85116	.06566	19.80028	6.61261	2.50130	.03188
128.13	190.78	1.25184	.07485	-.07416	-.01017	9.06867	10.2257	10.96010	.19720
128.13	195.78	1.28465	.08793	-.08771	-.00618	7.87657	10.5851	1.19390	.02389
128.13	200.78	1.31745	.06136	-.05744	.02157	10.4177	11.35037	-3.80553	-.05370
128.13	205.78	1.35026	.04403	.02494	.03629	16.51914	13.68203	-21.2989	-.15724
128.13	210.78	1.38307	.26927	.25488	.08687	25.51113	16.35219	-47.6925	-.19076
128.13	215.78	1.41588	.60338	.59169	.11817	27.40500	15.55227	-42.5340	-.16651
128.13	220.78	1.44869	.86430	.85195	.14556	19.55416	12.61711	-34.2120	-.23137
128.13	225.78	1.48150	.95470	.93940	.17024	10.41297	9.35208	-7.32089	-.12543
128.13	230.78	1.51430	.96179	.94677	.16929	5.10453	5.61351	-1.60976	-.09374
128.13	235.78	1.54711	.94655	.93101	.17080	3.36572	3.67189	.06288	.00849

Station 13 Wake Survey 0302WK13
Vref = 77.2924 m/s
Blade spacing (s) = 152.4 mm

x(mm)	y(mm)	y/s	W/Vref	U/Vref	V/Vref	Tu	Tv	Re Stress	Corr.
146.436	-14.218	-.09329	.90425	.89000	.15993	1.90560	1.91776	.57892	.26517
146.436	-9.220	-.06050	.90176	.88782	.15797	1.85627	1.80688	.39449	.19688
146.436	-4.220	-.02769	.89937	.88594	.15483	1.86386	1.75596	.26643	.13627
146.436	.780	.00512	.89897	.88605	.15186	1.73247	1.81579	.40267	.21427
146.436	5.780	.03793	.90239	.89018	.14793	1.75664	1.84838	.34463	.17766
146.436	10.780	.07073	.90840	.89656	.14619	1.91426	1.91257	.32185	.14715
146.434	15.780	.10354	.91875	.90734	.14433	1.94280	2.05716	.37087	.15533
146.436	20.780	.13635	.93878	.92695	.14858	2.24534	2.43875	.35052	.10715
146.436	25.782	.16917	.95989	.94711	.15614	2.96233	3.28209	.25877	.04455
146.436	30.780	.20197	.98066	.96668	.16499	5.26542	5.56742	1.47376	.08415
146.434	35.780	.23478	.89643	.86887	.22057	16.96140	11.60948	18.46060	.15693
146.436	40.780	.26759	.34183	.28797	.18417	22.40412	20.94161	95.60530	.34109
146.436	45.780	.30039	.07070	-.00058	.07070	13.0414	17.74707	23.13510	.16732
146.436	50.780	.33320	.02750	-.01006	.02560	13.3223	14.13875	-2.82791	-.02513
146.436	55.780	.36601	.08008	.07294	.03305	20.15167	13.84775	-8.28198	-.04968
146.434	60.780	.39882	.26410	.26041	.04400	25.36620	14.55826	-33.8942	-.15363
146.436	65.780	.43163	.53934	.53570	.06257	27.45113	14.44808	-46.3922	-.19580
146.436	70.780	.46444	.76891	.76428	.08427	22.45663	12.43298	-39.8770	-.23907
146.436	75.780	.49724	.88737	.88170	.10017	13.61427	9.13656	-11.4849	-.15455
146.436	80.780	.53005	.92520	.91787	.11623	6.36365	5.82751	-3.06727	-.13845
146.436	85.780	.56286	.91390	.90482	.12851	4.10460	3.92486	-.20270	-.02106
146.436	90.780	.59567	.90898	.89865	.13664	2.92599	2.66515	.26219	.05628
146.436	95.780	.62848	.90585	.89477	.14123	2.31959	2.12203	.07818	.02659
146.436	100.780	.66129	.89711	.88544	.14421	2.04358	1.97811	.34111	.14125
146.436	105.780	.69409	.89232	.87980	.14894	2.08018	1.82716	.37214	.16389
146.436	110.780	.72690	.88552	.87298	.14853	1.81552	1.69065	.31300	.17069
146.436	115.780	.75971	.88054	.86775	.14949	1.85318	1.62338	.22798	.12685
146.436	120.780	.79252	.87442	.86224	.14546	1.93049	1.62584	.42272	.22544
146.436	125.780	.82533	.87624	.86441	.14347	2.16406	1.68702	.23754	.10891
146.436	130.780	.85814	.87524	.86332	.14393	1.85967	1.55462	.38647	.22376
146.436	135.780	.89094	.87606	.86402	.14479	1.92936	1.61990	.36575	.19589
146.436	140.780	.92375	.87514	.86319	.14411	1.86605	1.71683	.50829	.26558
146.436	145.780	.95656	.87492	.86349	.14097	1.72325	1.67097	.28381	.16498
146.436	150.780	.98937	.87957	.86835	.14010	1.66321	1.60754	.34198	.21410
146.436	155.780	1.02218	.88181	.87074	.13929	1.66250	1.70821	.30531	.17995
146.436	160.780	1.05499	.88696	.87631	.13702	1.74410	1.89956	.36570	.18477
146.436	165.780	1.08780	.89312	.88307	.13363	1.82518	2.07236	.32310	.14299
146.436	170.780	1.12060	.90713	.89760	.13118	2.17945	2.38053	.66214	.21363
146.436	175.780	1.15341	.92617	.91622	.13540	2.43264	2.86558	.54029	.12974
146.436	180.780	1.18622	.94390	.93340	.14044	4.43944	4.49880	1.41597	.11867
146.436	185.780	1.21903	.92214	.90703	.16625	11.67425	9.08246	5.55523	.08770
146.436	190.780	1.25184	.54635	.49508	.23107	24.70367	19.44887	100.0720	.34865
146.436	195.780	1.28465	.13841	.06884	.12008	16.84408	21.39611	69.64920	.32349
146.436	200.780	1.31745	.06068	-.04738	.03792	10.85082	15.71384	12.89880	.12663
146.436	205.780	1.35026	.03086	-.02758	.01385	13.02651	13.19439	-8.76627	-.08537
146.436	210.780	1.38307	.08588	.08354	.01992	20.24772	13.58577	-15.0954	-.09186
146.436	215.780	1.41588	.26190	.25658	.05248	26.26535	14.59198	-20.9201	-.09137
146.436	220.780	1.44869	.50707	.50118	.07707	29.01797	15.32700	-69.7110	-.26236
146.436	225.782	1.48151	.73228	.72651	.09173	22.25297	12.62439	-41.4881	-.24720
146.436	230.780	1.51430	.87257	.86658	.10205	12.94646	10.08731	-19.7793	-.25352
146.436	235.780	1.54711	.90231	.89500	.11466	7.69240	7.37823	-8.53123	-.25161
146.436	240.780	1.57992	.90567	.89725	.12325	4.31988	4.39389	-.60585	-.05343

APPENDIX E.

STACK AND RVC3D CODE INPUTS

Input to Stack

```
&nl1 km=70 rhub=0.0 rtip=0.998 nblade=1 ysp=0.0071 dh1=0.01
   dt1=0.30 &end
```

Input to RVC3D

```
'GELDER CONTROLLED-DIFFUSION CASCADE'
&nl1 im=340 jm=49 km=70 itl=80 iil=143 &end
&nl2 cfl=5.0 avisc1=0.0 avisc2=0.0 avisc4=1.0 ivdt=1 nstg=4 itmax=7000
irs=1 epi=.60 epj=.70 epk=.70 &end
&nl3 ibcin=1 ibcex=1 isymt=1 ires=10 icrnt=50
iresti=0 iresto=1 ibcpw=0 iqin=0 &end
&nl4 emxx=0.16976 emty=0.13994 emrz=0.0 expt=0.0 prat=0.9729 ga=1.4
om=0.000000 igeom=0 alex= 9.0 &end
&nl5 ilt=2 tw=1.00 renr=6.0e5 prnr=.7 prtr=.9 vispwr=.666666
srtip=0.0 cmutm=10. jedge=30 kedge=50 iltin=2 dblh=2.5 dblt=0.00 &end
&nl6 io1=1 io2=340 oar=0 ixjb=0 njo=0 nko=0
jo=0 5 ko=0 &end
```

APPENDIX F.

OUTPUT FOR INLET AND EXIT CONDITIONS

****

j-direction averaged quantities on inlet
derived variables, absolute system
rho & ps are area-averaged, u, v, & w are momentum-averaged => approximate mixed-out average
notation: rr=rho0ref, cr=c0ref, er=rr*cr**2, pr=p0ref, tr=t0ref, alpha=atan(v/u), phi=atan(w/u)

****

k	distance	% mdot	vtot/cr	alpha	phi	ps/pr	p0/pr	ts/tr	t0/tr	Mach	p0 loss
1	0.00000	0.00000	0.00000	0.00000	0.00000	0.96846	0.96846	1.00000	1.00000	0.00000	0.00000
2	0.00267	0.00034	0.05901	56.02360	0.00000	0.96846	0.97083	0.99929	0.99999	0.05903	0.00000
3	0.00541	0.00128	0.08180	46.49279	0.00000	0.96816	0.97271	0.99865	0.99999	0.08185	0.00000
4	0.00821	0.00265	0.09594	41.84780	0.00000	0.96740	0.97366	0.99814	0.99998	0.09603	0.00000
5	0.01109	0.00432	0.10526	39.79194	0.00000	0.96686	0.97439	0.99776	0.99998	0.10538	0.00000
6	0.01403	0.00619	0.11125	38.99600	0.00000	0.96657	0.97499	0.99750	0.99997	0.11139	0.00000
7	0.01706	0.00821	0.11513	38.83252	0.00000	0.96648	0.97550	0.99732	0.99997	0.11529	0.00000
8	0.02016	0.01034	0.11778	38.96325	0.00000	0.96652	0.97596	0.99719	0.99997	0.11795	0.00000
9	0.02334	0.01257	0.11979	39.19616	0.00000	0.96660	0.97638	0.99710	0.99997	0.11997	0.00000
10	0.02660	0.01488	0.12152	39.42608	0.00000	0.96670	0.97676	0.99701	0.99997	0.12170	0.00000
11	0.02996	0.01728	0.12315	39.60389	0.00000	0.96678	0.97712	0.99694	0.99997	0.12334	0.00000
12	0.03340	0.01977	0.12477	39.71604	0.00000	0.96684	0.97745	0.99686	0.99997	0.12496	0.00000
13	0.03694	0.02237	0.12639	39.76921	0.00000	0.96687	0.97777	0.99678	0.99997	0.12660	0.00000
14	0.04058	0.02506	0.12802	39.77890	0.00000	0.96689	0.97806	0.99670	0.99997	0.12823	0.00000
15	0.04432	0.02787	0.12961	39.76194	0.00000	0.96689	0.97834	0.99662	0.99998	0.12983	0.00000
16	0.04817	0.03080	0.13115	39.73235	0.00000	0.96688	0.97861	0.99654	0.99998	0.13138	0.00000
17	0.05213	0.03385	0.13263	39.69987	0.00000	0.96686	0.97887	0.99646	0.99998	0.13287	0.00000
18	0.05621	0.03703	0.13404	39.67004	0.00000	0.96685	0.97911	0.99638	0.99998	0.13428	0.00000
19	0.06042	0.04033	0.13538	39.64513	0.00000	0.96684	0.97935	0.99631	0.99998	0.13563	0.00000
20	0.06475	0.04378	0.13665	39.62524	0.00000	0.96683	0.97958	0.99624	0.99998	0.13691	0.00000
21	0.06921	0.04736	0.13788	39.60940	0.00000	0.96683	0.97980	0.99618	0.99998	0.13814	0.00000
22	0.07382	0.05109	0.13905	39.59626	0.00000	0.96682	0.98002	0.99611	0.99998	0.13932	0.00000
23	0.07857	0.05497	0.14019	39.58458	0.00000	0.96681	0.98023	0.99605	0.99998	0.14047	0.00000
24	0.08348	0.05901	0.14129	39.57346	0.00000	0.96681	0.98044	0.99598	0.99998	0.14158	0.00000
25	0.08856	0.06321	0.14237	39.56239	0.00000	0.96681	0.98065	0.99592	0.99998	0.14266	0.00000
26	0.09380	0.06760	0.14342	39.55114	0.00000	0.96680	0.98085	0.99586	0.99998	0.14372	0.00000
27	0.09922	0.07216	0.14445	39.53969	0.00000	0.96679	0.98105	0.99581	0.99998	0.14476	0.00000
28	0.10483	0.07692	0.14546	39.52814	0.00000	0.96679	0.98125	0.99575	0.99998	0.14577	0.00000
29	0.11064	0.08188	0.14646	39.51661	0.00000	0.96678	0.98144	0.99569	0.99998	0.14677	0.00000
30	0.11666	0.08706	0.14744	39.50519	0.00000	0.96678	0.98163	0.99563	0.99998	0.14776	0.00000
31	0.12290	0.09247	0.14840	39.49396	0.00000	0.96677	0.98182	0.99557	0.99998	0.14873	0.00000
32	0.12937	0.09811	0.14935	39.48293	0.00000	0.96676	0.98201	0.99552	0.99998	0.14968	0.00000
33	0.13610	0.10401	0.15029	39.47211	0.00000	0.96676	0.98220	0.99546	0.99998	0.15063	0.00000
34	0.14308	0.11018	0.15122	39.46146	0.00000	0.96675	0.98238	0.99541	0.99998	0.15157	0.00000
35	0.15034	0.11663	0.15214	39.45096	0.00000	0.96674	0.98257	0.99535	0.99998	0.15249	0.00000
36	0.15789	0.12339	0.15305	39.44056	0.00000	0.96674	0.98276	0.99530	0.99998	0.15341	0.00000
37	0.16576	0.13047	0.15396	39.43025	0.00000	0.96673	0.98294	0.99524	0.99998	0.15433	0.00000
38	0.17396	0.13789	0.15487	39.42000	0.00000	0.96672	0.98313	0.99518	0.99998	0.15524	0.00000
39	0.18251	0.14568	0.15577	39.40977	0.00000	0.96671	0.98331	0.99513	0.99998	0.15615	0.00000
40	0.19144	0.15386	0.15667	39.39956	0.00000	0.96671	0.98350	0.99507	0.99998	0.15705	0.00000
41	0.20076	0.16246	0.15757	39.38934	0.00000	0.96670	0.98369	0.99502	0.99998	0.15796	0.00000

42	0.21052	0.17151	0.15847	39.37910	0.00000	0.96669	0.98388	0.99496	0.99998	0.15887	0.00000
43	0.22074	0.18104	0.15937	39.36880	0.00000	0.96668	0.98407	0.99490	0.99998	0.15978	0.00000
44	0.23146	0.19110	0.16027	39.35844	0.00000	0.96667	0.98426	0.99484	0.99998	0.16069	0.00000
45	0.24270	0.20171	0.16118	39.34799	0.00000	0.96666	0.98445	0.99478	0.99998	0.16161	0.00000
46	0.25451	0.21293	0.16210	39.33742	0.00000	0.96666	0.98465	0.99473	0.99998	0.16253	0.00000
47	0.26694	0.22480	0.16303	39.32671	0.00000	0.96665	0.98485	0.99467	0.99998	0.16346	0.00000
48	0.28004	0.23738	0.16396	39.31585	0.00000	0.96664	0.98505	0.99460	0.99998	0.16440	0.00000
49	0.29385	0.25073	0.16490	39.30480	0.00000	0.96663	0.98525	0.99454	0.99998	0.16535	0.00000
50	0.30844	0.26492	0.16586	39.29354	0.00000	0.96662	0.98546	0.99448	0.99998	0.16632	0.00000
51	0.32388	0.28003	0.16683	39.28205	0.00000	0.96660	0.98567	0.99441	0.99998	0.16730	0.00000
52	0.34025	0.29614	0.16782	39.27031	0.00000	0.96659	0.98589	0.99435	0.99998	0.16830	0.00000
53	0.35763	0.31335	0.16883	39.25830	0.00000	0.96658	0.98611	0.99428	0.99998	0.16931	0.00000
54	0.37611	0.33177	0.16985	39.24599	0.00000	0.96657	0.98634	0.99421	0.99998	0.17035	0.00000
55	0.39580	0.35153	0.17091	39.23337	0.00000	0.96655	0.98658	0.99414	0.99998	0.17141	0.00000
56	0.41684	0.37278	0.17199	39.22041	0.00000	0.96654	0.98682	0.99406	0.99998	0.17250	0.00000
57	0.43936	0.39567	0.17309	39.20712	0.00000	0.96652	0.98707	0.99399	0.99998	0.17362	0.00000
58	0.46352	0.42041	0.17424	39.19349	0.00000	0.96651	0.98733	0.99391	0.99998	0.17477	0.00000
59	0.48951	0.44721	0.17542	39.17957	0.00000	0.96649	0.98760	0.99383	0.99998	0.17597	0.00000
60	0.51754	0.47633	0.17665	39.16539	0.00000	0.96647	0.98789	0.99374	0.99998	0.17720	0.00000
61	0.54787	0.50807	0.17792	39.15096	0.00000	0.96646	0.98818	0.99365	0.99998	0.17849	0.00000
62	0.58080	0.54279	0.17925	39.13609	0.00000	0.96644	0.98849	0.99355	0.99998	0.17983	0.00000
63	0.61666	0.58093	0.18065	39.12027	0.00000	0.96642	0.98882	0.99345	0.99998	0.18125	0.00000
64	0.65587	0.62298	0.18213	39.10266	0.00000	0.96639	0.98917	0.99335	0.99998	0.18274	0.00000
65	0.69892	0.66957	0.18370	39.08276	0.00000	0.96637	0.98955	0.99323	0.99998	0.18432	0.00000
66	0.74641	0.72146	0.18536	39.06297	0.00000	0.96634	0.98995	0.99311	0.99998	0.18601	0.00000
67	0.79906	0.77955	0.18709	39.05466	0.00000	0.96632	0.99038	0.99298	0.99998	0.18775	0.00000
68	0.85776	0.84494	0.18879	39.08606	0.00000	0.96634	0.99085	0.99285	0.99998	0.18947	0.00000
69	0.92361	0.91891	0.19030	39.20073	0.00000	0.96645	0.99136	0.99273	0.99998	0.19099	0.00000
70	0.99800	1.00000	0.19080	39.23853	0.00000	0.96649	0.99153	0.99269	0.99998	0.19150	0.00000
***** overall averages **											
71	0.49900	0.15339	0.17298	39.22453	0.00000	0.96654	0.98706	0.99408	1.00007	0.17349	0.00000

****

j-direction averaged quantities on exit

derived variables, absolute system

rho & ps are area-averaged, u, v, & w are momentum-averaged => approximate mixed-out average

notation: rr=rho0ref, cr=c0ref, er=rr*cr**2, pr=p0ref, tr=t0ref, alpha=atan(v/u), phi=atan(w/u)

****

k	distance	% mdot	vtot/cr	alpha	phi	ps/pr	p0/pr	ts/tr	t0/tr	Mach	p0 loss
1	0.00000	0.00000	0.00000	0.00000	0.00000	0.97290	0.97290	0.99999	0.99999	0.00000	0.02710
2	0.00267	0.00031	0.03056	-7.45493	0.03446	0.97290	0.97354	0.99979	0.99997	0.03056	0.02646
3	0.00541	0.00118	0.05509	-7.36759	0.00552	0.97290	0.97497	0.99937	0.99997	0.05511	0.02503
4	0.00821	0.00252	0.07399	-7.25528	-0.01744	0.97290	0.97664	0.99889	0.99998	0.07403	0.02336
5	0.01109	0.00425	0.08813	-7.11798	-0.03393	0.97290	0.97821	0.99845	1.00000	0.08820	0.02179
6	0.01403	0.00629	0.09855	-6.96094	-0.05049	0.97290	0.97954	0.99808	1.00002	0.09864	0.02046
7	0.01706	0.00858	0.10613	-6.78754	-0.06780	0.97290	0.98061	0.99779	1.00004	0.10624	0.01939
8	0.02016	0.01109	0.11154	-6.59779	-0.08591	0.97290	0.98142	0.99756	1.00005	0.11168	0.01858
9	0.02334	0.01376	0.11530	-6.38985	-0.10461	0.97290	0.98201	0.99740	1.00006	0.11545	0.01799
10	0.02660	0.01658	0.11778	-6.16158	-0.12360	0.97290	0.98241	0.99729	1.00007	0.11794	0.01759
11	0.02996	0.01954	0.11926	-5.91188	-0.14263	0.97290	0.98265	0.99722	1.00007	0.11943	0.01735
12	0.03340	0.02260	0.11998	-5.64131	-0.16157	0.97290	0.98277	0.99718	1.00006	0.12015	0.01723
13	0.03694	0.02577	0.12015	-5.35223	-0.18041	0.97290	0.98279	0.99717	1.00006	0.12032	0.01721
14	0.04058	0.02902	0.11994	-5.04806	-0.19923	0.97290	0.98276	0.99717	1.00005	0.12011	0.01724
15	0.04432	0.03237	0.11949	-4.73239	-0.21816	0.97290	0.98269	0.99718	1.00004	0.11966	0.01731
16	0.04817	0.03581	0.11895	-4.40837	-0.23737	0.97290	0.98260	0.99720	1.00003	0.11912	0.01740
17	0.05213	0.03934	0.11840	-4.07855	-0.25703	0.97290	0.98251	0.99722	1.00002	0.11857	0.01749
18	0.05621	0.04296	0.11792	-3.74494	-0.27729	0.97290	0.98243	0.99723	1.00001	0.11808	0.01757

19	0.06042	0.04669	0.11754	-3.40912	-0.29828	0.97290	0.98237	0.99724	1.00001	0.11770	0.01763
20	0.06475	0.05052	0.11729	-3.07238	-0.32011	0.97290	0.98233	0.99725	1.00000	0.11745	0.01767
21	0.06921	0.05446	0.11717	-2.73562	-0.34284	0.97290	0.98231	0.99725	1.00000	0.11733	0.01769
22	0.07382	0.05853	0.11716	-2.39916	-0.36648	0.97290	0.98231	0.99725	1.00000	0.11733	0.01769
23	0.07857	0.06274	0.11726	-2.06255	-0.39101	0.97290	0.98232	0.99725	1.00000	0.11743	0.01768
24	0.08348	0.06708	0.11745	-1.72450	-0.41638	0.97290	0.98235	0.99724	1.00000	0.11761	0.01765
25	0.08856	0.07158	0.11769	-1.38302	-0.44252	0.97290	0.98239	0.99723	1.00000	0.11785	0.01761
26	0.09380	0.07624	0.11797	-1.03604	-0.46937	0.97290	0.98244	0.99721	1.00000	0.11814	0.01756
27	0.09922	0.08107	0.11828	-0.68187	-0.49685	0.97290	0.98249	0.99720	1.00000	0.11845	0.01751
28	0.10483	0.08608	0.11860	-0.31928	-0.52490	0.97290	0.98254	0.99719	1.00000	0.11877	0.01746
29	0.11064	0.09128	0.11893	0.05262	-0.55346	0.97290	0.98260	0.99717	1.00000	0.11910	0.01740
30	0.11666	0.09668	0.11927	0.43440	-0.58245	0.97290	0.98265	0.99716	1.00000	0.11944	0.01735
31	0.12290	0.10230	0.11960	0.82641	-0.61182	0.97290	0.98270	0.99714	1.00000	0.11977	0.01730
32	0.12937	0.10813	0.11994	1.22879	-0.64149	0.97290	0.98276	0.99713	1.00001	0.12011	0.01724
33	0.13610	0.11421	0.12028	1.64157	-0.67136	0.97290	0.98282	0.99712	1.00001	0.12046	0.01718
34	0.14308	0.12053	0.12064	2.06481	-0.70132	0.97290	0.98288	0.99710	1.00001	0.12082	0.01712
35	0.15034	0.12712	0.12101	2.49835	-0.73126	0.97290	0.98294	0.99709	1.00002	0.12119	0.01706
36	0.15789	0.13399	0.12140	2.94176	-0.76105	0.97290	0.98300	0.99707	1.00002	0.12158	0.01700
37	0.16576	0.14116	0.12182	3.39423	-0.79060	0.97290	0.98307	0.99706	1.00002	0.12200	0.01693
38	0.17396	0.14865	0.12226	3.85473	-0.81983	0.97290	0.98315	0.99704	1.00003	0.12244	0.01685
39	0.18251	0.15648	0.12274	4.32197	-0.84869	0.97290	0.98323	0.99702	1.00003	0.12293	0.01677
40	0.19144	0.16468	0.12326	4.79438	-0.87719	0.97290	0.98332	0.99699	1.00003	0.12345	0.01668
41	0.20076	0.17327	0.12382	5.27007	-0.90535	0.97290	0.98341	0.99697	1.00004	0.12401	0.01659
42	0.21052	0.18229	0.12442	5.74678	-0.93330	0.97290	0.98352	0.99694	1.00004	0.12461	0.01648
43	0.22074	0.19177	0.12506	6.22180	-0.96119	0.97290	0.98363	0.99691	1.00004	0.12525	0.01637
44	0.23146	0.20174	0.12574	6.69196	-0.98923	0.97290	0.98374	0.99688	1.00004	0.12594	0.01626
45	0.24270	0.21224	0.12646	7.15372	-1.01773	0.97290	0.98387	0.99685	1.00005	0.12666	0.01613
46	0.25451	0.22333	0.12722	7.60327	-1.04700	0.97290	0.98400	0.99681	1.00005	0.12742	0.01600
47	0.26694	0.23504	0.12799	8.03682	-1.07750	0.97290	0.98414	0.99677	1.00005	0.12820	0.01586
48	0.28004	0.24744	0.12878	8.45103	-1.10986	0.97290	0.98428	0.99673	1.00005	0.12899	0.01572
49	0.29385	0.26058	0.12956	8.84368	-1.14499	0.97290	0.98442	0.99669	1.00005	0.12977	0.01558
50	0.30844	0.27453	0.13031	9.21451	-1.18379	0.97290	0.98455	0.99665	1.00005	0.13052	0.01545
51	0.32388	0.28934	0.13100	9.56664	-1.22868	0.97290	0.98468	0.99662	1.00005	0.13123	0.01532
52	0.34025	0.30509	0.13159	9.88626	-1.28193	0.97290	0.98478	0.99659	1.00005	0.13182	0.01522
53	0.35763	0.32185	0.13201	10.14582	-1.34402	0.97290	0.98486	0.99657	1.00005	0.13224	0.01514
54	0.37611	0.33967	0.13225	10.32509	-1.41326	0.97290	0.98490	0.99656	1.00006	0.13247	0.01510
55	0.39580	0.35865	0.13233	10.41270	-1.48424	0.97290	0.98492	0.99657	1.00007	0.13256	0.01508
56	0.41684	0.37887	0.13236	10.40686	-1.54783	0.97290	0.98492	0.99658	1.00008	0.13258	0.01508
57	0.43936	0.40046	0.13242	10.31474	-1.59170	0.97290	0.98494	0.99659	1.00009	0.13265	0.01506
58	0.46352	0.42360	0.13265	10.15019	-1.60214	0.97290	0.98498	0.99659	1.00011	0.13288	0.01502
59	0.48951	0.44851	0.13315	9.93015	-1.56696	0.97290	0.98507	0.99657	1.00012	0.13338	0.01493
60	0.51754	0.47552	0.13398	9.67118	-1.47887	0.97290	0.98522	0.99653	1.00012	0.13421	0.01478
61	0.54787	0.50504	0.13519	9.38806	-1.33798	0.97290	0.98545	0.99646	1.00012	0.13543	0.01455
62	0.58080	0.53759	0.13682	9.09526	-1.15267	0.97290	0.98576	0.99636	1.00010	0.13707	0.01424
63	0.61666	0.57381	0.13891	8.80923	-0.93853	0.97290	0.98615	0.99622	1.00008	0.13917	0.01385
64	0.65587	0.61444	0.14147	8.54851	-0.71573	0.97290	0.98665	0.99606	1.00006	0.14175	0.01335
65	0.69892	0.66030	0.14442	8.33010	-0.50528	0.97290	0.98724	0.99587	1.00004	0.14472	0.01276
66	0.74641	0.71231	0.14757	8.16412	-0.32497	0.97290	0.98788	0.99567	1.00003	0.14789	0.01212
67	0.79906	0.77148	0.15060	8.05064	-0.18596	0.97290	0.98850	0.99548	1.00002	0.15094	0.01150
68	0.85776	0.83886	0.15312	7.98126	-0.09066	0.97290	0.98904	0.99533	1.00002	0.15348	0.01096
69	0.92361	0.91561	0.15479	7.94465	-0.03275	0.97290	0.98940	0.99523	1.00002	0.15516	0.01060
70	0.99800	1.00000	0.15536	7.93298	0.00000	0.97290	0.98952	0.99519	1.00002	0.15574	0.01048
***** overall averages **											
71	0.49900	0.15346	0.13682	7.28813	-0.69505	0.97290	0.98576	0.99634	1.00008	0.13707	0.01424

LIST OF REFERENCES

1. Gelder, T. F., Schmidt, J. F., Suder, K. L., and Hathaway, M. D., "Design and Performance of Conrolled-Diffusion Stator Compared With Original Double-Circular-Arc Stator", NASA Technical Paper 2852, March 1989.

2. Sanger, N. L., and Shreeve, R. P., "Comparison of Calculated and Experimental Cascade Performance for Controlled-Diffusion Compressor Stator Blading", *ASME Journal of Turbomachinery*, Vol. 108, July, 1986.

3. Hansen, D. J., "Investigation of Second Generation Controlled-Diffusion Compressor Blades in Cascade", Master's Thesis, Naval Postgraduate School, Monterey, California, September, 1995.

4. Schnorenberg, D. G., "Invetigation of the Effect of Reynolds Number on Laminar Separation Bubbles on Controlled-Diffusion Compressor Blades in Cascade", Master's Thesis, Naval Postgraduate School, Monterey, California, June, 1996.

5. Elazar, Y., "A Mapping of the Viscous Flow Behavior in a Controlled Diffusion Compressor Cascade Using Laser Doppler Velocimetry and Preliminary Evaluation of Codes for the Prediction of Stall", Ph.D. Dissertation, Naval Postgraduate School, Monterey, California, March, 1988.

6. Webber, M. A., "Determining The Effect Of Endwall Boundary Layer Suction in a Large Scale Subsonic Compressor Cascade", Master's Thesis, Naval Postgraduate School, Monterey, California, March, 1993.

7. Classick, M. A., "Off-Design Loss Measurements in a Compressor Cascade", Master's Thesis, Naval Postgraduate School, Monterey, California, September, 1989.

8. Armstrong, J. H., "Near-Stall Loss Measurements in a CD Compressor Cascade With Exploratory Leading Edge Flow Control", Master's Thesis, Naval Postgraduate School, Monterey, California, September, 1990.

9. Murray, K. D., "Automation and Extension of LDV Measurements of Off-Design Flow in a Subsonic Cascade Wind Tunnel", Master's Thesis, Naval Postgraduate School, Monterey, California, June, 1989.

10. Chima, R.V., "RVC3D (Rotor Viscous Code 3-D) User's Manual and Documentation", NASA Lewis Research Center, March, 1992.

BIBLIOGRAPHY

1. Sanger, N. L., "The Use of Optimization Techniques to Design Controlled-Diffusion Compressor Blading", *ASME Journal of Engineering for Power*, Vol. 105, 1986.

2. Elazar, Y., and Shreeve, R. P., "Viscous Flow in Controlled Diffusion Compressor Cascade with Increasing Incidence", *ASME Journal of Turbomachinery*, Vol. 112, April 1990.

3. Hobson, G. V., Williams A. J. H., and Rickel H. H., "Laser-Doppler Velocimetry Measurements In a Cascade of Compressor Blades At Stall", ASME Paper No. 96-GT-484, Gas Turbine and Aeroengine Congress and Exhibition, Birmingham, UK, June 10-13, 1996.

4. Hobson, G. V., and Shreeve, R. P., "Inlet Turbulence Distortion and Viscous Flow Development in a Controlled-Diffusion Compressor Cascade at Very High Incidence", *Journal of Propulsion and Power*, Vol. 9, No. 3, May-June, 1993.

INITIAL DISTRIBUTION LIST

1. Defense Technical Information Center 2
   8725 John J. Kingman Road., Ste 0944
   Ft. Belvoir, VA 22060-6218

2. Dudley Knox Library 2
   Naval Postgraduate School
   411 Dyer Rd.
   Monterey, CA 93943-5101

3. Chairman 1
   Department of Aeronautics and Astronautics
   Code AA/Li
   Naval Postgraduate School
   699 Dyer Road - Room 137
   Monterey, CA 93943-5106

4. Professor R. P. Shreeve. 1
   Department of Aeronautics and Astronautics
   Code AA/Sf
   Naval Postgraduate School
   699 Dyer Road - Room 137
   Monterey, CA 93943-5106

5. Assoc. Professor G. V. Hobson. 7
   Department of Aeronautics and Astronautics
   Code AA/Hg
   Naval Postgraduate School
   699 Dyer Road - Room 137
   Monterey, CA 93943-5106

6. Naval Air Warfare Center - Aircraft Division. 1
   Code Air - 4.4.3.1 [S. McAdams]
   Propulsion and Power Engineering, Bldg. 106
   Patuxent River, MD 20670-5304

7. Mr. Darren V. Grove 1
   13805 Fritz Drive S.W
   Cumberland, MD. 21502